ALMA MATER STUDIORUM - UNIVERSITÀ DI BOLOGNA

SCHOOL OF ENGINEERING AND ARCHITECTURE

Department of
Electrical, Electronic and Information Engineering
"Guglielmo Marconi"
DEI

Electrical Engineering

MASTER THESIS
in
Photovoltaic Conversion and Storage of the Electrical Energy

MODELING AND MODEL VALIDATION OF SUPERCAPACITORS FOR REAL-TIME SIMULATIONS

Presented by: Supervisor:

Simone Pezzolato   Prof. Dr.-Ing. Antonio Morandi

                                                                                  Co-Supervisors:

                                                                                  Shahab Karrari

                                                                    Dr. Giovanni De Carne

                                                          Prof. Dr.-Ing. Mathias Noe

                                                          Prof. Dr.-Ing. Pierluigi Ribani

Academic Year 2018/2019
Session III

Table of Content

Table of figures

Table of Tables

Table of Equations

Abstract

Supercapacitors are becoming very important in the automotive and energy and power industry due to their specially characteristics, in particular in the field of hybrid vehicles and hybrid energy storage systems. For this reason, having accurate models that can represent the behavior of such systems is necessary and the main important characteristics of supercapacitor are a high-power density and a long lifetime with low maintenance. This thesis focuses on modeling supercapacitors to the study of their behavior in a short time period. As, their operation often short intense power deliveries. The goal of this thesis is to compare the accuracy of equivalent-circuit models of supercapacitors together with their required execution time for real-time simulations.

In the first chapter, the operation of the supercapacitor from the molecular point of view and the principal of storing energy in a supercapacitor is introduced. Common operation modes of supercapacitors are also introduced. Next, equivalent-circuit models of supercapacitors are introduced. The models are implemented in MATLAB/Simulink and their responses are compared with the experimental results. The parameter estimation results. The parameter estimation tool of MATLAB has been used to estimate the model parameters for each model. At the end, the models are compared in terms of inaccurately reproducing the experimental response of a supercapacitor. Lastly, the models are compared in terms of their required execution time for real-time simulations. The models are implemented in RT-LAB software and simulated on the Opal-RT's OP4510 real-time simulator. Here the execution times of the models compared with the goal of representing a large number of supercapacitor cells.

1 Chapter 1: Introduction to Supercapacitors

1.1 Structure and Operation Principle

The supercapacitor is a system composed by two metallic collectors in the extreme parts. These collect and distribute the current. Going toward the center there are porous carbon made electrodes (μm), then the electrolyte. In the mid of the electrolyte there is a separator, permeable for ions, in order to not have a short circuit among electrodes. The schematic of a supercapacitor cell is shown in Figure 1.1 [1].
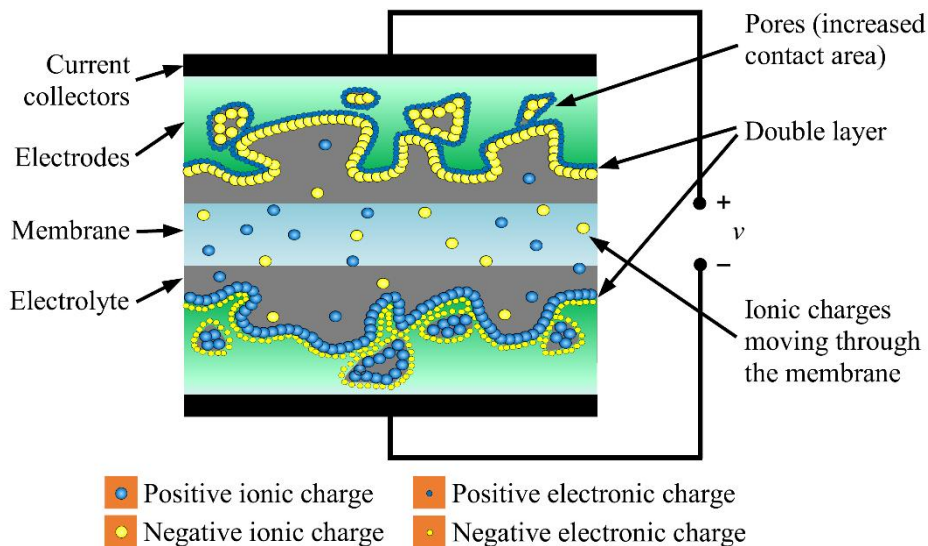
Figure 1.1 Schematic of a supercapacitor cell

1.1.1 Molecular point of view

The structure is similar to that one of a battery, but it has not reacting materials.

In the batteries there is a plate charging negatively because there is a natural oxidation reaction: some atoms lose their electrons leaving them in the electrode. They are now available for the conduction and take part to the adjacent solution. In the cathode occurs the opposite reaction: some atoms

acquire the electrons. This charge configuration will create its own potential configuration. There is a potential gradient; in the middle the potential remains constant being the electrolyte an inert conductor and finally there is another gradient. The voltage on the system is the no-load voltage across the electrochemical battery (ΔV).

In the building of a supercapacitor, cause the use of inert materials, positive and negative ions remain randomly located. There is not charge thickening and so there is not a voltage across terminals. However, applying a voltage across the component a current is generated and some electrons leave an electrode going toward the other. This is a physical charge shifting. A plate is charging positively, and negative ions thickening around occurs. Electrons carried by the electromotive force in the other plate charge it negatively. Close to this electrode positive ions are attracted. A double charge layer is created, like a capacitor. It is like to have the positive charges distribution (being part of the electrode structure), the negative charges distribution in the electrolyte made by anions and cations with absorbed molecules. A negative ion has around solvent polar molecules. This molecule has both positive and negative parts, but it is globally neutral but with different barycenter for positive and negative charge. This is an electric dipole interacting with the cation surrounding it.

This set of surrounded particles go close to the electrode staying yet at a distance of a molecular layer called "Double Layer" ($\approx 10^{-10} m$). In the detail, this can tell us that being the distance very low, the capacitance will be high. The surface is also affecting the capacitance. In fact, the surface is very huge due to porous carbon. Its surface is full of irregularities. These make the final value much greater.

1.1.2 Energy storage

This structure is called "Helmholtz Double Layer". This is represented by a series of a capacitor, a resistance and finally another capacitor. There are also two parallel resistances in parallel with the two capacitors, representing the self-discharge behavior on those interfaces.
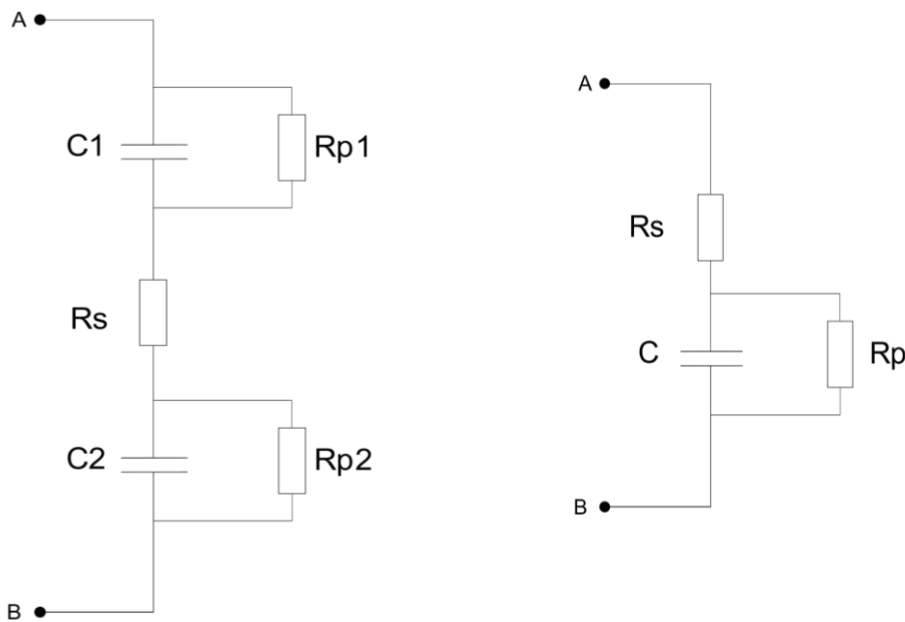
Figure 1.2 Helmholtz Double Layer model (left), Model of the Supercapacitor (right)

The equivalent circuit is summed up to a capacitance with a parallel resistance, and an equivalent series resistance playing a basic role in the efficiency of the component. This simplification is since the two RC parallels are almost similar, so the current splitting can be represented in a unique parallel. Every capacitance is given by:

$$C = \frac{\varepsilon \cdot S}{d}$$

1.1

Where is it 'ε' is the permittivity of the dielectric, 's' is the surface and 'd' is the distance. So, the capacitance will be high having a very low distance ($\approx \mu m$) and a very high surface given by the porous carbon, into which the liquid conductor leaches. There are lot of holes in the powder that is enough compact to create an electric continuity and at the same time to increase the surface by means of the great deal of holes ($S \approx 3000 \; m^2/cell$).

For example, a Maxwell BCAP (Cn=3000F, Vn=2.7V, ESR=0.29mΩ) has

$$W_n = \frac{1}{2}CV^2 = 10,9kJ \approx 3Wh$$

This value is the rated energy stored in the capacitor.

A capacitor can be used till his voltage is remaining higher than a threshold value, which usually is the half of the rated voltage

$$V_{min} = \frac{1}{2}V_n$$

1.2

So, the available energy is

$$\Delta W = \frac{1}{2}CV_n{}^2 - \frac{1}{2}CV_{min}{}^2 = 75\% \; W_n$$

1.3

1.2 Applications of Supercapacitor Energy Storage Systems

Large applications for supercapacitors can be found in microgrids. Renewable sources are in great expansion due to the environmental impact which is one of the issues to which many countries pay close attention. The production targets with renewable sources are of great importance and the management of these systems goes hand in hand with their expansion. The problem with renewable sources is that they do not guarantee constant energy production over time. This in turn is a source of

great problems for electricity grids because it is the cause of continuous electricity quality

disturbances. Moreover, it affects the stability and reliability of the systems. Microgrids, in

particular, are small systems that can be connected directly to the network or operate in an islanded

manner. They often integrate large amounts of ESS. These networks need both great energy and

great power density: this is why often just one ESS is not enough, so we get to use more than one of

these systems together. This gives rise to HESSs (Hybrid Energy Storage Systems).

Figure 1.3 shows four configurations of ESS. Figure 1.3a)[2] and Figure 1.3b)[3] represent simpler

topologies, while Figure 1.3c) and Figure 1.3d) represent more complex systems [4]. In particular,

hybrid storage systems constituted of Vanadium Redox Batteries (VRB) and supercapacitors,

connected to energy production systems with Permanent Magnets Synchronous Machine (PMSM).
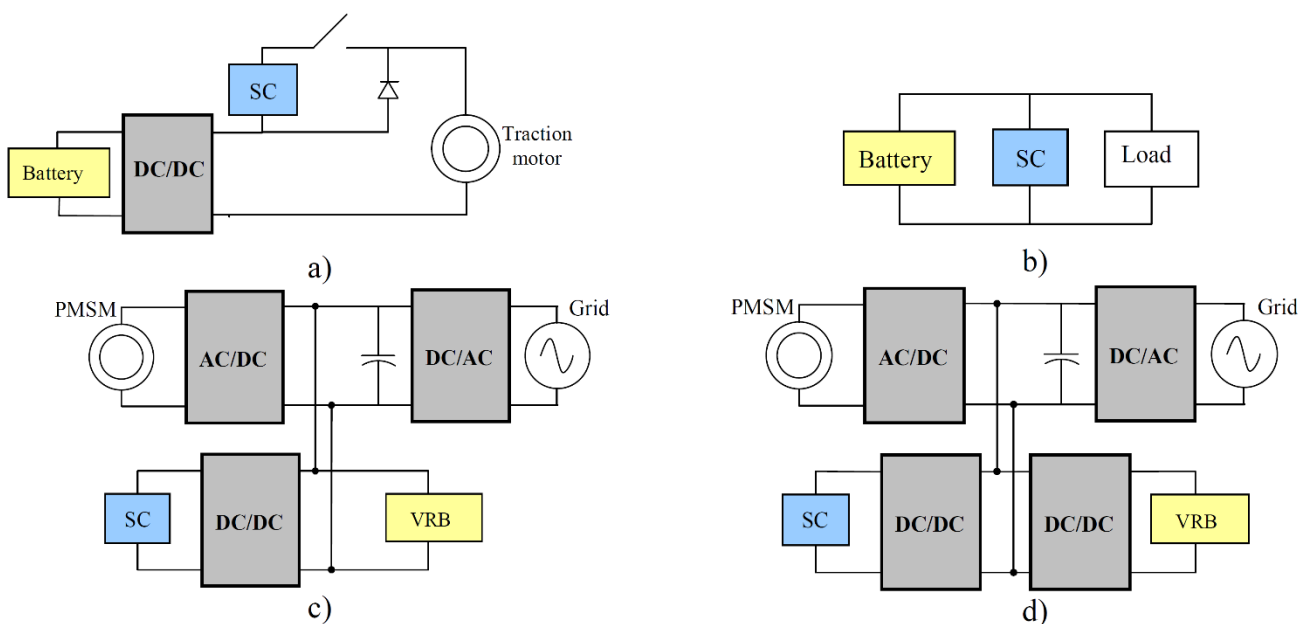
Figure 1.3 Examples of topologies using supercapacitors to have a more performant ESS: a) Series topology; b) Parallel passive topology; c) Parallel active topology (direct connection of ESS to the DC bus); d) Parallel active topology (both ESS with a PCS) .

The contribution of supercapacitors is very important as they are sources of high-power density in a

short time, while other systems deal with the amount of energy in longer times. Energy management

is very important in these microgrids. There are converters, which require particular attention in the

construction choices, and an energy optimization system is always needed in order to better coordinate the microgrid. This gives the possibility to better meet the requirements of stability and good functioning of the network [5].

SCs are also used in UPSs because they offer performance that batteries cannot achieve. Often the two are used together. Indeed, SCs can provide energy during short outages better than batteries. In addition, this will extend the life of the batteries. Sometimes UPSs also have only supercapacitors, because with sensitive loads they are sufficient and have lower maintenance costs.

The SCs can be used as energy recovery means for elevators and cranes. In fact, in these cases the energy can be recovered in the downward phases. The supercapacitors are therefore adequate because they allow energy recovery in a short time and are able to supply large currents which is what is needed in these applications.

The automotive industry is also an area in which SC are increasingly taking hold. Here too, as in the previous cases, it is possible to combine the use with batteries. Their use varies from low energy consumption applications to applications with a higher energy level. Their combination with batteries offers numerous advantages, including greater power, greater energy recovery and longer battery life thanks to the leveling of charge cycles. This is a leading sector for the use of supercapacitors as a booming sector [6].

1.3 Common operation modes of supercapacitors

The voltage response of the supercapacitor is analyzed using the equivalent circuit with a capacitance and series resistance shown in Figure 1.4. The parallel resistance is neglected, because it is taking into
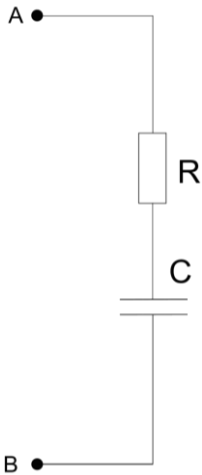
Figure 1.4 RC series equivalent circuit of a supercapacitor cell

account the self-discharge phenomena acting in a very long-time scale $(Rp \approx \Omega \rightarrow \tau = Rp \cdot C \approx 3000s)$. Other supercapacitor models will be discussed in the next chapter.

1.3.1 Constant current

Here the supercapacitor is subjected to constant current charge-discharge cycles. The current i will be a square wave, with set both amplitude and duty-cycle. The component receives the current and what interesting is the voltage response across the supercapacitor. The initial voltage is the minimum voltage of such component, that typically is $\frac{V_n}{2}$. This is the voltage allowing the correct performing of the converter linked to the supercapacitor. Where there is no input current, the voltage remains constant. The component would be affected by the self-discharge phenomena but, as already said, that phenomena will be neglected.

Once a positive pulse of current is applied, the voltage value is immediately observable.

It is a vertical increment due to the series resistor, and the voltage has a value $R_s \cdot i$, as it can be seen in Figure 1.5.
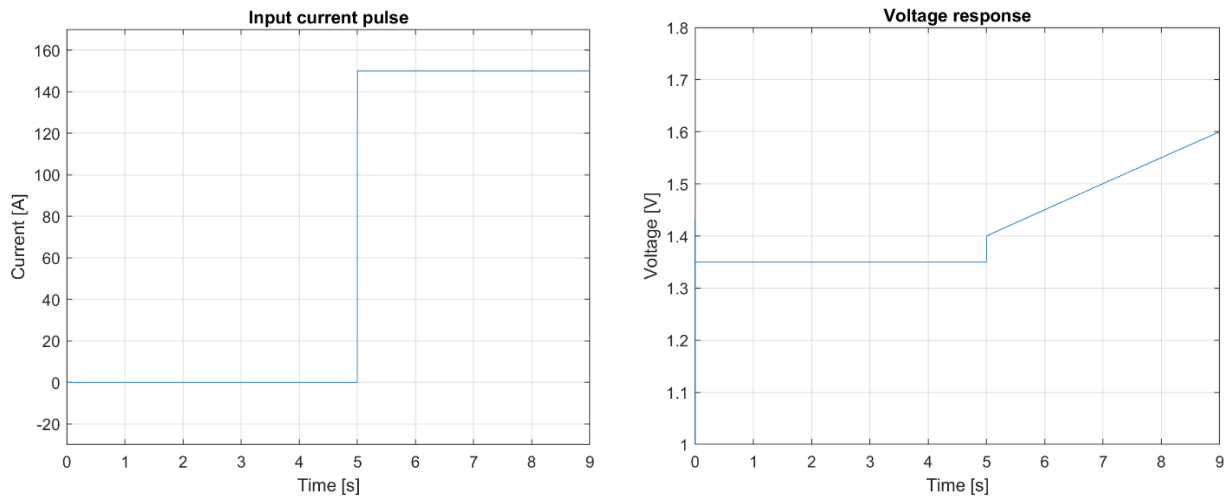
Figure 1.5 ESR is responsible for the voltage step that occurs across the SC

When the current is applied the voltage of the supercapacitor increases. Input current pulses and voltage response are shown in Figure 1.6. The law governing this part is $i_c = C \cdot \dfrac{d}{dt} V_c$ and the voltage across the supercapacitor is
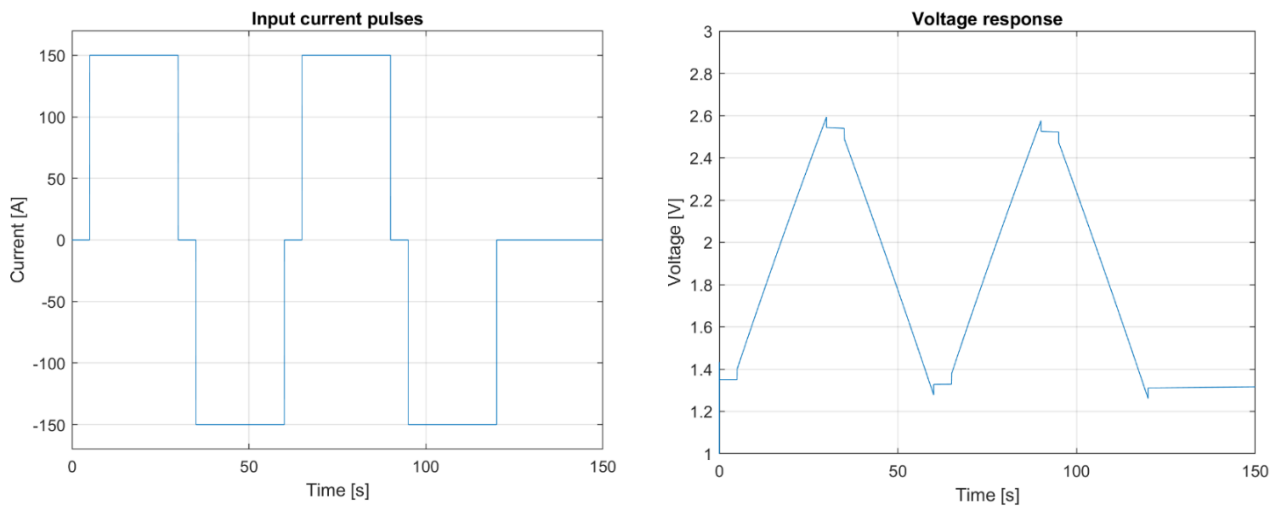
Figure 1.6 Voltage response of the supercapacitor with the shown input current pulses

$$V = v_{co} + R_s \cdot i + \frac{1}{C} \cdot \int i_c dt \qquad \qquad 1.4$$

The current pulse continues at the high value. Once arrived at the rated voltage value the current turn down to 0A. Now is shown a vertical step. This is still due to the voltage drop of the series resistor. Now the voltage tends to remain constant. This happens because no energy is released out of the supercapacitor and the charge inside remains constant (self-discharge neglected). Length of pulses is not known a priori because it is something depending on the application. Now starting to inject a negative current pulse, equal and opposite to the positive first one; now it is like to have the circuit in Figure 1.7 (discharge phase):
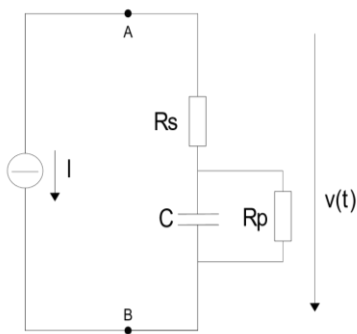
Figure 1.7 Equivalent circuit for the discharging phase

The value of the current is given by the total voltage across the supercapacitor. During charge, starting from $\frac{V_n}{2}$, a constant current i is injected till the voltage arrives at V_n, and here the current turn off; during the discharge, the input current is provided with the same amplitude and opposite sign. The voltage begins to drop with the same slope with which it previously went up. In fact, assuming constant capacitor, the slope will always be the same. In the discharge phase current stops once reached $\frac{V_n}{2}$. At the moment when current is imposed, there is a small jump due to the resistance. The

voltage drop due to resistance occurs every time the current will be applied. Being the constant current, the power will vary linearly as the voltage. Analyzing in detail a single period (i.e. including a charge and a discharge) we can see that the areas determined by the performance of the power are not equal: in fact, the area described by the SC discharge will be smaller. This is due to the fact that part of the energy is lost due to internal resistance.

It is possible to analyze the effect of the ESR from the efficiency point of view.

By assuming the equivalent circuit of Figure 1.7

$$V = V_c + R_s \cdot i \qquad\qquad 1.5$$

$$V \cdot i = V_c \cdot i_c + R_s \cdot i^2 \qquad\qquad 1.6$$

$$V \cdot i = V_c \cdot C \cdot \frac{dV_c}{dt} + R_s \cdot i^2 \qquad\qquad 1.7$$

$$t_a < t < t_0 \rightarrow discharge \qquad\qquad 1.8$$
$$t_b < t < t_c \rightarrow charge \qquad\qquad 1.9$$

Energy injected in the supercapacitor in the charge time:

$$E_{in} = \frac{1}{2}C(V_{cb}{}^2 - V_{ca}{}^2) + R_s \cdot i^2(t_b - t_a) \qquad\qquad 1.10$$

The second term of the equation represents the energy lost cause of the series resistance.

Estimation of charge and discharge times:

$$\Delta t = C\Delta V_c = C\left(\frac{V_n - R_s \cdot i - \left(\frac{V_n}{2} + R_s \cdot i\right)}{i}\right) = C\frac{\left(\frac{V_n}{2} + 2R_s \cdot i\right)}{i} \qquad\qquad 1.11$$

Efficiency:

$$\eta = \frac{E_{out}}{E_{in}} = \frac{\Delta W_c - R_s \cdot i^2 \cdot \Delta t_{scarica}}{\Delta W_c + R_s \cdot i^2 \cdot \Delta t_{scarica}} < 1$$

ΔW = supercapacitor internal energy variation

$R_s \cdot i^2 \cdot \Delta t$ = Joule losses

What it is injected in the supercapacitor during the charge, is then extracted during the discharge. The difference is the voltage across the resistance. An energy that is never extracted is dissipated. With higher power, the efficiency will result to be lower, due to the higher current over a constant series resistance. In Figure 1.7 is shown the efficiency variation as function of the current. Equation 1.12 shows that the efficiency is dependent on the current and on the ESR. In fact, increasing the current particularly, the term $\Delta R_s \cdot i^2 \cdot \Delta t_{scarica}$ increases, and the efficiency decreases. The voltage and the current affect the power. Increasing the current the power increases. In Figure 1.8 are shown two power curves as function of voltage and current.
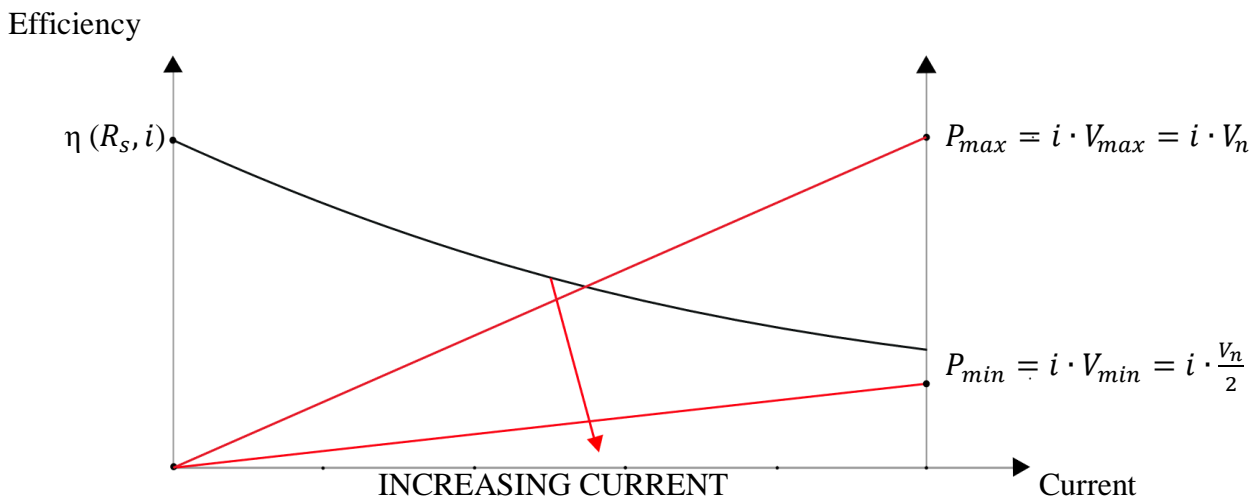
Figure 1.8 Supercapacitor efficiency in a constant current operation

17

So, it is possible to see that working at higher powers the efficiency decreases because the current required is greater and the drop on the ESR increases. Exploiting cells in terms of power forces you to give up something from the point of view of performance.

1.3.2 Constant power

A constant power charge-discharge cycle is analyzed. Here are applied two initial conditions: both series and parallel resistances are neglected.

The control regulates the current to have a constant power. The power is positive when it is injected and negative when it is extracted from the SC. In the initial instant there is the minimum voltage (half of the rated voltage). Also, in this case the voltage never drops below half the rated voltage.

The current of the supercapacitor is controlled in order to obtain the constant power operation.

$$p = v \cdot i = v_c \cdot i \qquad\qquad 1.13$$

$$i = C \frac{dv_c}{dt} \qquad\qquad 1.14$$

So, from these two equations:

$$p = C v_c \frac{dv_c}{dt} \qquad\qquad 1.15$$

Now integrating and supposing a constant applied from t=0, it is obtained

$$\frac{1}{2} C \left(V^2 - V_0{}^2\right) = \pm p(t - t_0) \qquad\qquad 1.16$$

Before the injection there is zero power and so zero current. Then it started to be injected a constant power. The injected power is positive and the extracted one is negative as shown in Figure 1.10. At the initial moment it is $V_0 = V_{min}$ and it is possible to continue inserting power in the supercapacitor till the maximum voltage. In the same way it is possible to pick out power from the supercapacitor until half the rated voltage. Figure 1.9 shows the voltage trend, starting from half the rated voltage and increasing as long as current is injected.
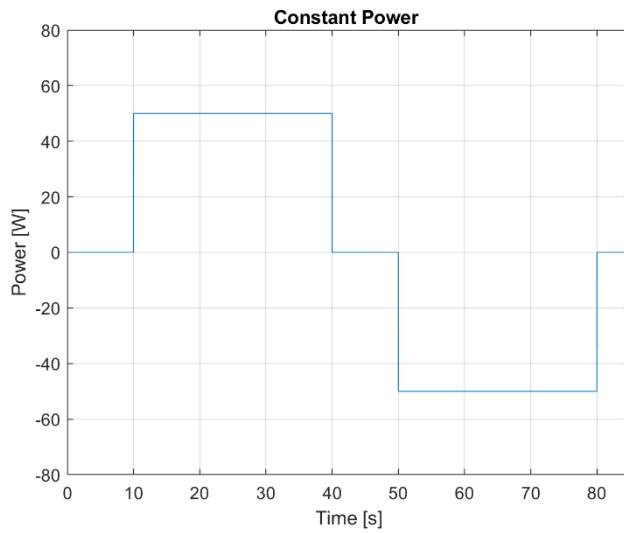
Figure 1.10 Constant power injection and extraction

The voltage across the component ideally follow the below relation

$$V = \sqrt{V_0{}^2 \pm \frac{2p}{C}(t - t_0)}$$
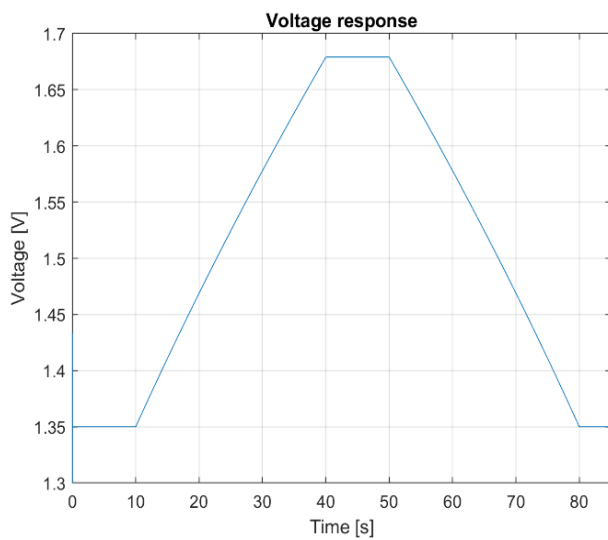
Figure 1.9 Voltage behaviour with constant power neglecting the ESR

The positive for the charge, the negative during the discharge. Now the voltage is varying, and the power is constant. A constant power means that the current has to vary because the product of

19

current and voltage must supply a constant quantity. This means that the current has to decrease to maintain the power constant. The current trend is shown in Figure 1.11. It can be seen that the voltage varies with the square root of time and so the current decrease with the same trend, as shown in Figure 1.11. When the maximum voltage is reached, the injection will no longer take place. And the same goes for the minimum voltage. Once the extraction is reached, it must be blocked so as not to drop below the threshold (this is to allow the converter to adequately control the power exchanged).
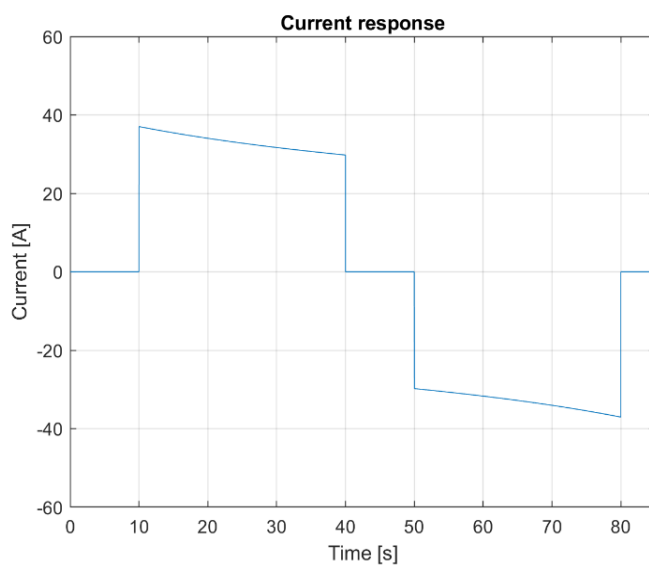
Figure 1.11 Current behaviour with constant power

It can be seen that by inserting and extracting power in the SC the voltage will increase and decrease. But being the power constant, it means that the current will vary because the product of current and voltage.

So, starting from the initial instant, the required power is zero therefore the current will also have a zero value. Then the charging phase starts then, the injected current starts from the value $i = \frac{p}{V_{min}}$.

At the beginning of the charge the voltage is equal to the minimum voltage value (nominal voltage) therefore the current will start from the value $i = \frac{p}{V_{min}}$. During the charging phase then the voltage

will rise, and consequently the current will have to decrease to keep the power constant. Once the

charging phase is over, the current will have a value of $i = \frac{p}{V_{max}}$, a non-linear increase of the current

from the initial to the final value is obtained. This is due to the fact that the voltage, grows with the

square root of time (see Figure 1.12). The same thing happens for the discharge phase. The current

starts from a minimum value and then increases to the maximum value when the voltage is half the

nominal.

This is the operation neglecting the serious resistance, but its effect cannot be overlooked.

Now let's see the behavior considering also the series resistance.

In the same way we start with zero power and zero current. Once the power injection has started,
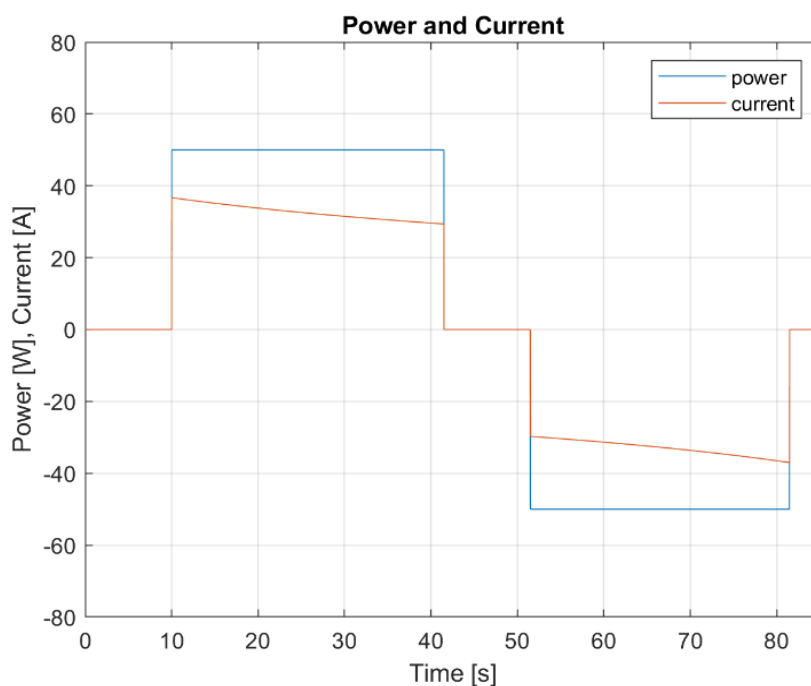
Figure 1.12 Power and Current in the first cycle

having the voltage at the minimum value (half of the rated voltage) we will have the maximum

current. Here the voltage drop on the resistance will therefore be maximum, as shown in Figure 1.14.

As you can see, in the first case the voltage drop is just over 0.012V, while in the second case it is around 0.01V.
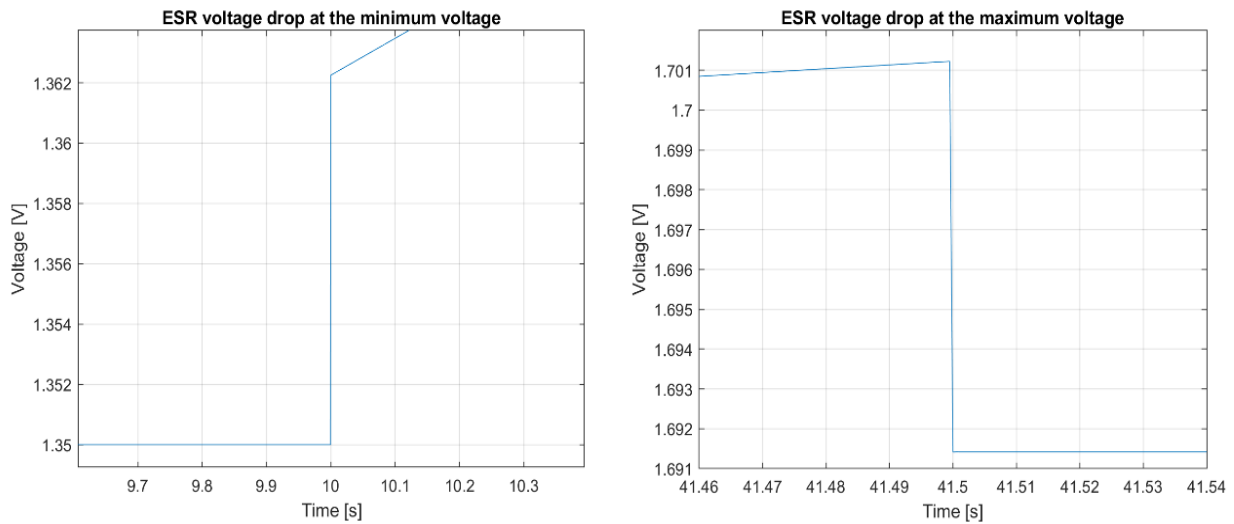
Figure 1.14 ESR voltage drop difference: on the left the drop at minimum voltage is represented instead on the right that one at the maximum voltage

In Figure 1.13 can be observed that the voltage rises with the same trend until it reaches the maximum voltage. Once the maximum value is reached, the power injection will stop and therefore the current will also stop. Here again I have a voltage drop which, however, will be less due to the fact that
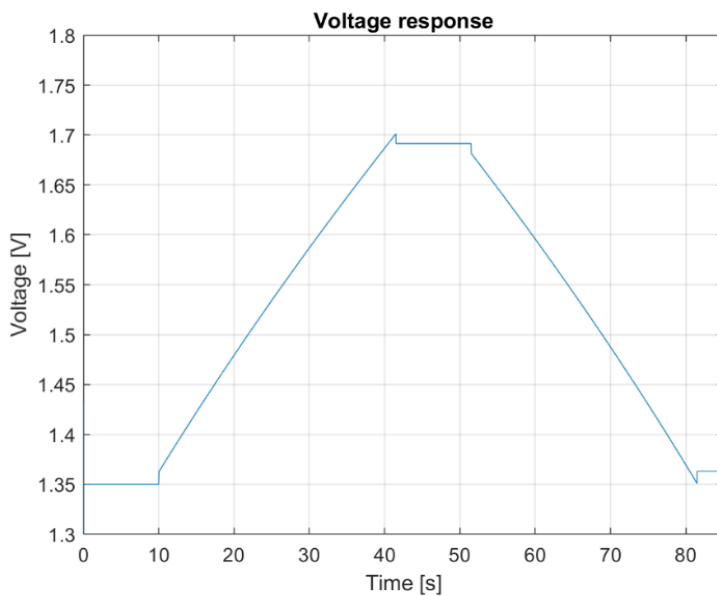
Figure 1.13 Voltage response taking into account the ESR

when the voltage is maximum the current is minimum therefore the voltage drop will be smaller than

that experienced when the charging phase began.
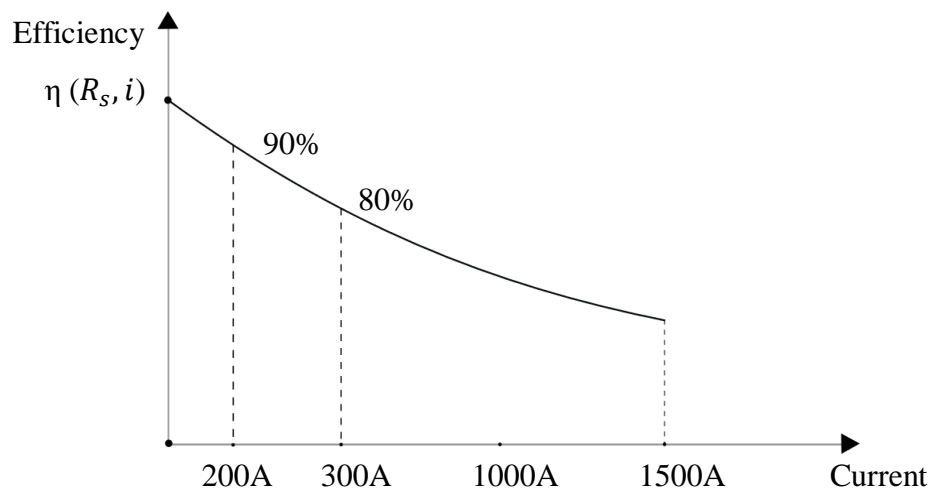
Figure 1.15 Efficiency as function of the current

The performance trend shows that a reasonable operating regime for the cell is around 100W.

For high powers the efficiency decreases, and the use of multiple cells must be considered.

2 Chapter 2: Modeling of Supercapacitor Cells

For modeling of a supercapacitors, we start by model of single cell. In the literature, there are two main types of cell models, i.e. the physics-based models and equivalent circuit model. The focus of this work is on the equivalent circuit models that are approximations voltage-current characteristic of the cell. These models do not necessarily reflect the chemical actions inside the cell, but their can replicate the cells response with high accuracy. The cell model should have the following characteristics:

• Accurate enough to represent a real supercapacitor cell, in particular in transient behavior

• Simple enough for real-time simulations.

• Suitable for the time scale of the study (seconds to minutes)

2.1 Equivalent-circuit Modeling of Supercapacitors

In this chapter, some of the most famous models of supercapacitors are introduced. The modeling of the component is addressed from different points of view, starting from the molecular aspect up to what concerns its most macroscopic behavior. The latter is the one on which the thesis will be focused and therefore models that develop the molecular aspect of the component will not be considered. In literature, several models for supercapacitors are introduced, from which four models have been identified for the purpose of this work. These are

- The RC series model
- The Two-Branch model
- The Zubieta model
- The Series model

Excluding the RC model which only gives a simplified representation of the component's behavior, the other models are more accurate due to the fact that they present a breakdown of the time constant within a cell, dividing its representation into several branches. Note that the value of the capacitance of the models may in general depend on the voltage. This aspect is fundamental to a better representation of the behavior of the supercapacitor cell. In fact, the capacitance value tends to vary as voltage varies.

2.1.1 The RC series model

The first model to be examined is the RC series model shown in Figure 2.1. This is the simplest model, widely used for the approximate analysis of the cell behavior as in the previous chapter. The RC series model only introduce one time constant governing the dynamic of the cell which is simply given by the product of the resistance and the capacitance of the cell, i.e. $\tau = R \cdot C$
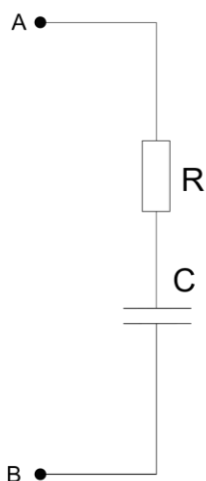
Figure 2.1 RC model

This model is used to have a general overview of the component's behavior. It should be noted that this model does not take into account the self-discharge phenomenon as there is only one resistance in the model. This is one of the disadvantages of this model. It also cannot accurately represent

charging and discharging cycles with accuracy. In the latter there are voltage variations increasing and decreasing of the voltage that cannot be adequately represented with this model. On the other hand, however, this model has a great advantage which is its simplicity [7].

2.1.2 The Two-Branch model

This model is more complex than the previous one. In fact, the Two Branch model, shown in Figure 2.2, is a model in which a subdivision of the time constant takes place [8]. The circuit consists of several branches in which the representation of the component dynamics is divided.

Note that the first branch is composed of a resistance and a variable capacitor. This capacitor is the sum of two terms: a constant one and a voltage dependent one. The capacitance of this branch is the main accumulation component while the resistance of this branch is the one that acts as Equivalent
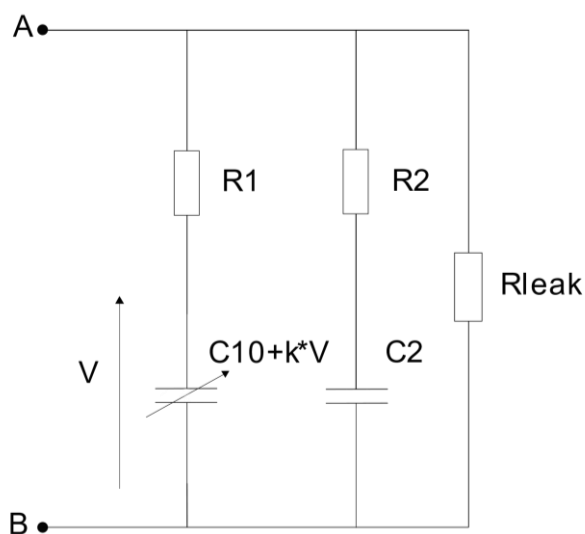
Figure 2.2 The Two-Branch model

Series Resistance (ESR). This branch is the one with the fastest dynamics. The second branch represents the medium-long term and is in the order of magnitude of minutes. The second branch does not contain variable terms. The third and final branch is that which represents the phenomenon

of self-discharge. This term is actually relevant for the complete representation of the component. However, this model is used for representations of a generally shorter period and, as in the case in question, it will not be considered. In this work, we simplify this model by eliminating the third branch and obtaining the model of Figure 2.3 .

Increasing capacitor as voltage increases means that the stored energy also increases.
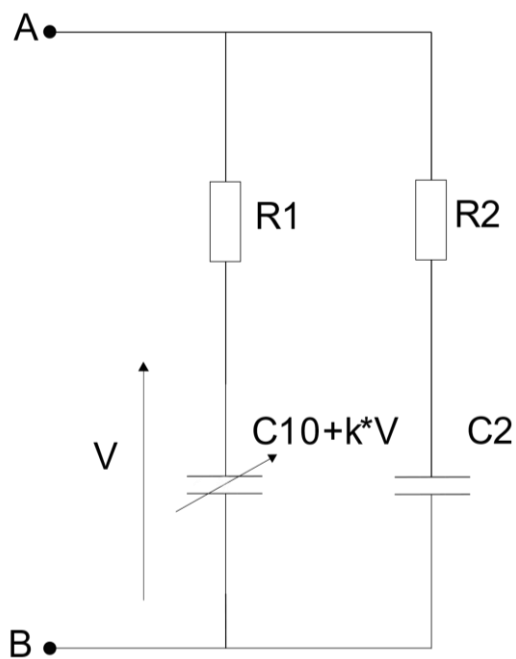
Figure 2.3 Simplified Two-Branch model

2.1.3 The Zubieta model

The third model is the Zubieta model shown in Figure 2.4 [9]. This model is very similar to the previous (Two-Branch model). In fact, also this model, we have a subdivision of the various dynamics of the component through multiple branches and the first branch has a variable capacitor. In particular, it can be seen that the first branch is composed of a series resistor (R1), which

represents the ESR. In series with the resistance there is the main capacitor consisting of two terms (C10, k*V) just like for the Two-Branch model. The first term will be constant and the second will depend on the voltage across the capacitor. The two components are in parallel, so the two capacitor values are added together. This branch defines the behavior of the circuit in the first few seconds. The second branch is composed of a resistance and a series capacitor (R2, C2). This branch has a time constant in the order of a few minutes. The third branch consisting of resistance and capacitor (R3, C3) has a time constant of over tens of minutes. Finally, the last branch represents the phenomenon of self-discharge. In this model the last branch is considered because, being a model with a greater distribution of the dynamics of the system for our purpose it should be made up of all
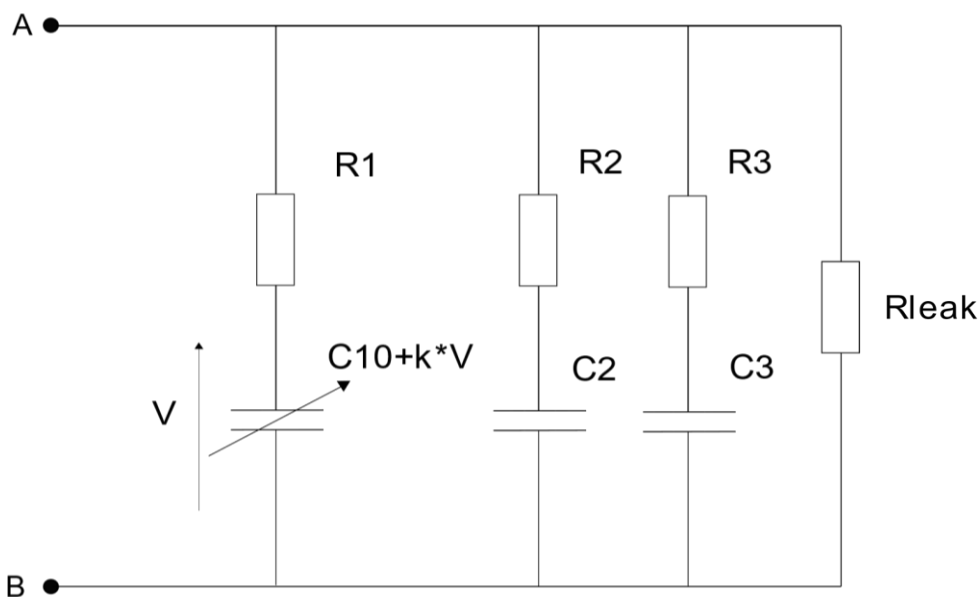
Figure 2.4 The Zubieta model

its branches. In fact, this model should represent the behavior of the supercapacitor in a span of 30 minutes.

The timing is therefore longer than the two-branch model which should be based on fewer minutes.

2.1.4 The Series model

The series model is the most complex of the four taken into consideration. It is shown in Figure 2.5. It is made up of a large amount of components, many of which are variable with time [10]. This makes it a heavy and difficult model to implement. Also, reliable and robust identification of parameters is very complex. The peculiarity of this model is linked to the first branch. In fact, here we find a large subdivision of the time constant through parallels of resistance and capacitor. Each block of a parallel of resistance and capacitor, we call a block. In this work, five blocks are used to get a good model accuracy. Remember that the first branch deals with the faster dynamics of the system. It can be noted that in the first branch only the series resistance (equivalent of the ESR of the component) is a constant parameter while all the others are variable parameters. In series with the above-mentioned resistance we find a capacitor which is the main storage component. This is composed of a fixed part and a variable part.
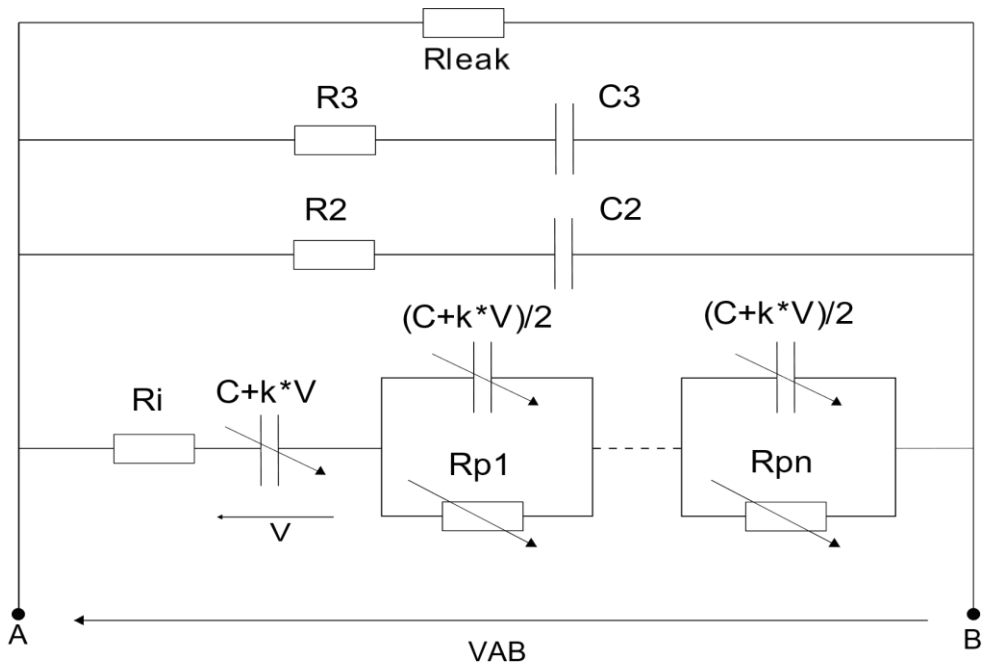
Figure 2.5 The Series model

The variable part of each capacitance is obtained multiplying the voltage by a constant (k). In each block, is inserted half the value of the total capacitance given by summing fix and variable part.

The lookup table is a component used in Simulink to have voltage dependent components. In the case in question, it is calculated from 0 to the rated voltage (2.7V) as shown in Figure 2.6.
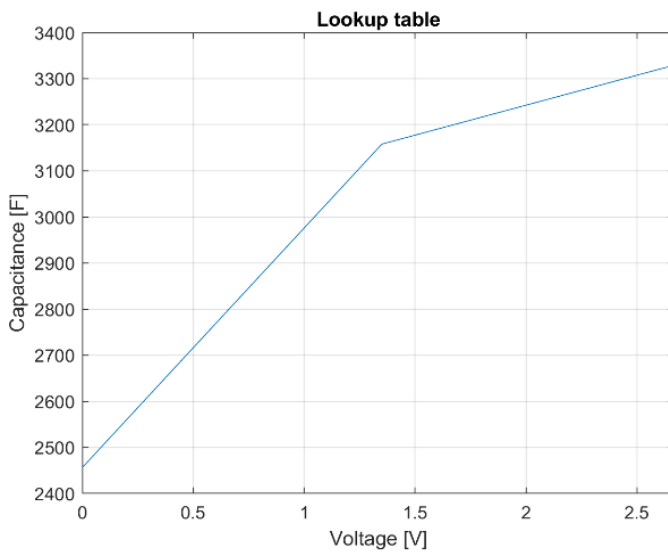
Figure 2.6 Example of Lookup-table

An interpolation is also made for the resistance placed parallel to the capacitor of each block. The resistance value of each block descends with $\frac{1}{n_{block}}$, in which n_{block} is the number of the block, following Equation 2.1. In that equation can be seen how every block has a different resistance. The time constant of each block decreases for each subsequent block. This is in order to accurately represent the fast dynamics of the system.

The equation of the parallel resistance of the blocks follows. In the blocks the reference resistor value is scaled for every block. Note that it decreases with the square of the block number (n).

$$R_{pn} = \frac{2 \cdot \tau(V)}{n^2 \pi^2 C(V)}$$
2.1

So, once the behavior of the first branch has been defined, we find three other branches: now there is a lot of similarity with the Zubieta model in that each branch defines a time constant. Each parameter has a constant value just like the previous model. The last branch takes into account the self-discharge phenomenon.

2.2 Model Validation

2.2.1 Description of Supercapacitor

The supercapacitor cell that is considered for modeling is a Maxwell supercapacitor. All the cell data are shown below, directly from the data sheet provided by the manufacturer.

Table 2.1 Main characteristics of the supercapacitor cell considered	
ELECTRICAL	BCAP3000
Rated Capacitance	3000F
Minimum Capacitance, initial	3000F
Maximum Capacitance, initial	3600F
Maximum ESRDC, initial	0.29mΩ
Test Current for Capacitance and ESR_{DC}	100 A
Rated Voltage	2.70 V
Absolute Maximum Voltage	2.85 V
Absolute Maximum Current	1900 A
Leakage Current at 25° C, maximum	5.2 mA
TEMPERATURE	
Operating temperature (Cell case temperature)	
Minimum	-40° C
Maximum	65° C
Storage Temperature (Stored uncharged)	
Minimum	-40° C
Maximum	70° C
PHYSICAL	
Mass, typical	510g
Terminals	Threaded or Weldable

Maximum Terminal Torque (K04)	14 Nm
Vibration Specification	ISO 16750, Table 14
Shock Specification	SAE J2464
POWER & ENERGY	BCAP3000
Usable Specific Power, P_d	5,900 W/kg
Impedance Match Specific Power, P_{max}	12,000 W/kg
Specific Energy, E_{max}	6.0 Wh/kg
Stored Energy, E_{stored}	3.04 Wh
SAFETY	
Short Circuit Current, typical (Current possible with short circuit from rated voltage. Do not use as an operating current.)	9,300 A
Certifications	UL810a, RoHS

TYPICAL CHARACTERISTICS

THERMAL CHARACTERISTICS	
Thermal Resistance (R_{ca}, Case to Ambient), typical8	3.2o C/W
Thermal Capacitance (C_{th}), typical	600 J/o C
Maximum Continuous Current ($\Delta T = 15°$ C)	130 ARMS
Maximum Continuous Current ($\Delta T = 40°$ C)	210 ARMS
LIFE	
DC Life at High Temperature (held continuously at Rated Voltage and Maximum Operating Temperature)	1,500 hours
Capacitance Change (% decrease from minimum initial value)	20%
ESR Change (% increase from maximum initial value)	100%

Projected DC Life at 25° C (held continuously at Rated Voltage)	10 years
Capacitance Change (% decrease from minimum initial value)	20%
ESR Change (% increase from maximum initial value)	100%
Projected Cycle Life at 25°C	1000000cycles
Capacitance Change (% decrease from minimum initial value)	20%
LIFE	
ESR Change (% increase from maximum initial value)	100%
Test Current	100A
Shelf Life (Stored uncharged at 25° C)	4 years

Table 2.1 Product specifications

Figure 2.7 shows the capacitance behavior as function of the temperature:
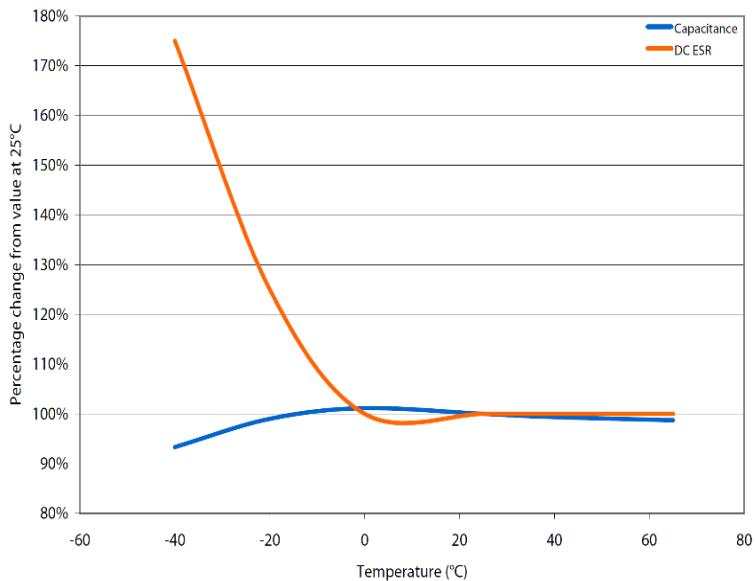
Figure 2.7 ESR and Capacitance as function of the temperature. Courtesy of picture: Maxwell Technologies

it can be noted that optimal operation can be obtained between about 0 ° C and an ambient

temperature of around 25 ° C. In this range it is possible to obtain the maximum capacitor and have

an ESR that varies around the minimum value as shown in Figure 2.7. This is something that is

important from the point of view of performance as it is this resistance value that particularly influences it. The structure of the supercapacitor cell is described in Figure 2.8 and Figure 2.9. Dimensions are shown in Table 2.2.
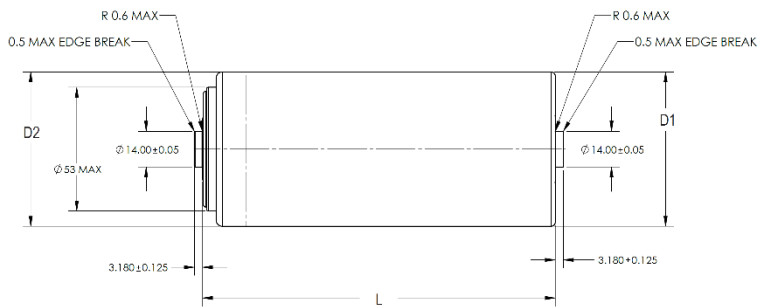
Figure 2.8 Cell structure from data-sheet. Courtesy of picture: Maxwell Technologies

Dimensions (mm)				
Part description	L (±0.3mm)	D1 (±0.2mm)	D2 (±0.7mm)	Package Quantity
BCAP3000 P270 K04/05	138	60.4	60.7	15

Table 2.2 Dimensions of the supercapacitor cell
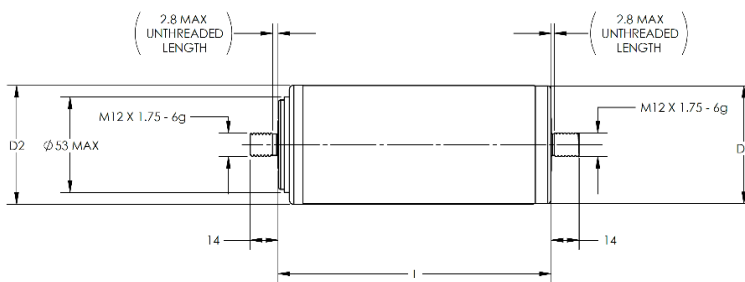
Figure 2.9 Cell structure from data-sheet(2). Courtesy of picture: Maxwell Technologies

2.2.2 Experimental Setup

Here, the experimental setup and procedure of the supercapacitor cell is explained. Two-quadrant operation of the supercapacitor has been made possible by:
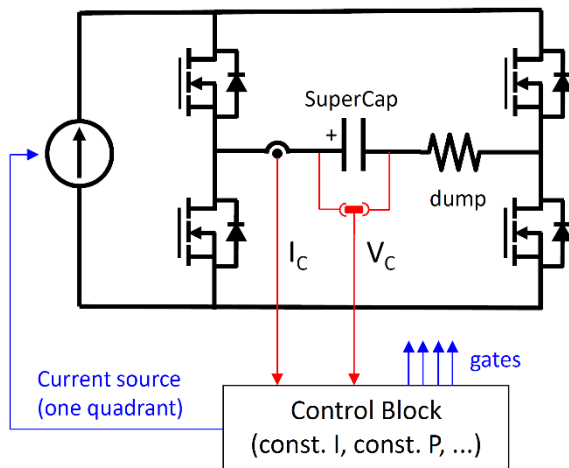
Figure 2.10 Experiment setup

- One-quadrant TDK Lambda GEN8 (400A – 8V), current source, and dump resistor
- Power MOSFET inverters
- Labview management system

Feedback control of source current allowing the two important operation modes:

- Constant current cycling
- Constant power cycling

The component is tested by carrying out charging and discharging cycles at constant current on it.

The start is from half of its rated voltage, so in this case it is 1.35V as shown in Figure 2.11. The test
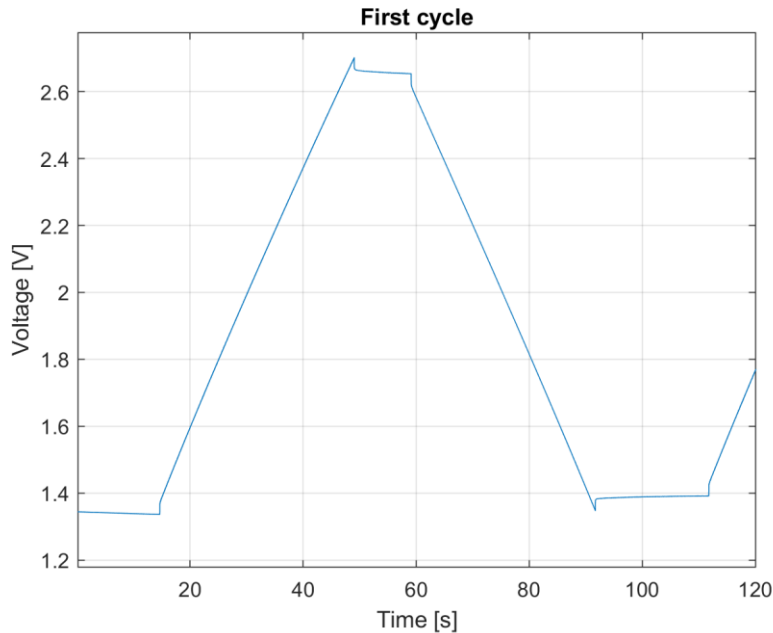
Figure 2.11 Shift got after the first cycle.

will take place symmetrically with positive and negative current pulses in a periodic way (see Figure

2.12). The first cycle has an asymmetry due to ESR which causes an increase in voltage from the

second cycle onwards. This occurs because what controls the insertion of current into the component

is its voltage level. By starting to inject a positive current, the charging phase of the first cycle will

end when the rated voltage is reached (2.7V in the case under consideration). Once at nominal

voltage the current value will go to zero. before the discharge phase there are 10s of waiting. Then

the discharge phase begins, and the voltage begins to decrease. It is important to note that the

sequence of moments in which ESR influences causes the initial voltage of each cycle following the

first to be greater than the initial voltage at the instant t =0. There is a 20s off period before the next

positive impulse. This process is repeated up to having four charge-discharge cycles. Thus we note

that our component is kept cyclically charged for 10s. The voltage then decreases until it reaches half
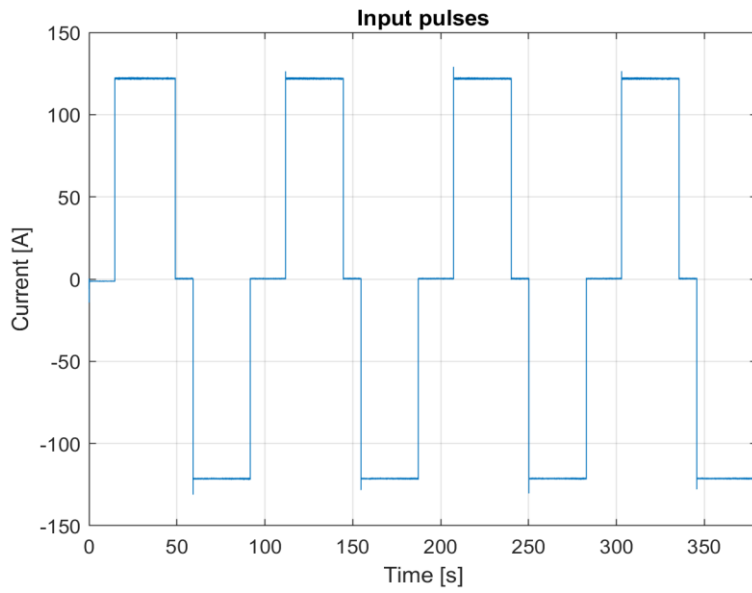
Figure 2.12 Input current pulses sequence.

the rated voltage where the current returns to 0. Four charge and discharge cycles are applied. There

is a 20s off period before the new positive impulse. And so, on up to having four charge-discharge
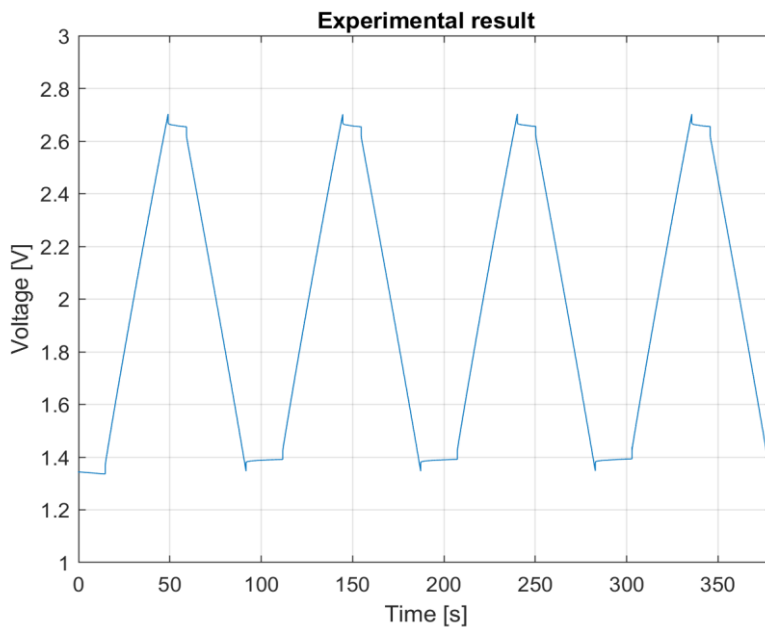
Figure 2.13 Voltage measured across the component during the experiment

cycles. Thus, we note that our component is kept cyclically charged for 10s. So what we get is the

live response shown in Figure 2.13.

2.2.3 Parameter Estimation Procedure

Now, knowing the response of the component, we will proceed with the estimation of the parameters of the models that have been introduced. The supercapacitor models are (apart from the RC model) quite complex, in particular the series model. To obtain all the parameters of each model, the MATLAB/Simulink parameter estimation tool was used to estimate the parameters. This tool allows, with the input and output data, to estimate each parameter of the circuit. The circuits are implemented in MATLAB/Simulink. The experimental data are voltage and current values. These are inserted into the tool. In the toolbox it is also possible to define a range, so that the parameters can vary but in a limited way (i.e. within the range). Once the conditions in which the parameters will be estimation are set, the estimate is carried out. During the estimation it will be possible to monitor the execution of the model as, at each variation the model runs to verify the actual accuracy of the variation.
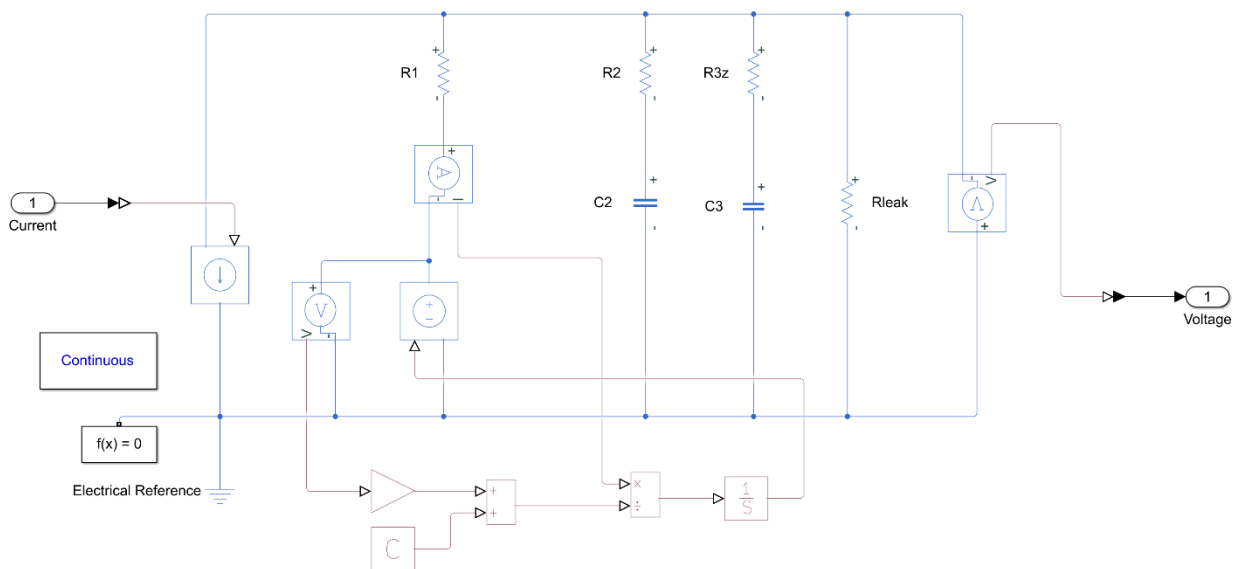
Figure 2.14 Simulink model of the Zubieta model

We then proceed with the estimation of the parameters of each model. This process involves different computation times for each model depending on its complexity. What may also affect the starting conditions of the estimate. Obviously if the entered parameters from which the estimate is already close to the final values, the estimation process will be faster because it will require less iteration to arrive at the solution. In fact, the achievement of a correct estimation depends on the value of the parameters at the beginning of the estimate. The more complex the model, the more local optimums can be found during the estimation process. This can lead to an incorrect estimate of the parameters which therefore will not allow the model to respond better.

2.2.4 Comparison between Models

The first model analyzed is the RC model. It is the lightest cause made up of only two parameters.
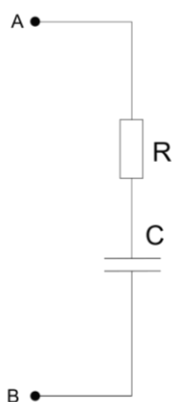
Figure 2.15 The RC model

Parameter	Value
R	0.41407 mΩ
C	3139.3 F

Table 2.3 The estimated parameters for the RC model

It can be noted that the estimated parameters are not too different from those reported by the manufacturer. Now, to verify the actual quality of the parameter estimation of the model, the output of the model will be compared with the measurement. The comparison is shown in Figure 2.16 In this way it is possible to see if the model answers correctly.
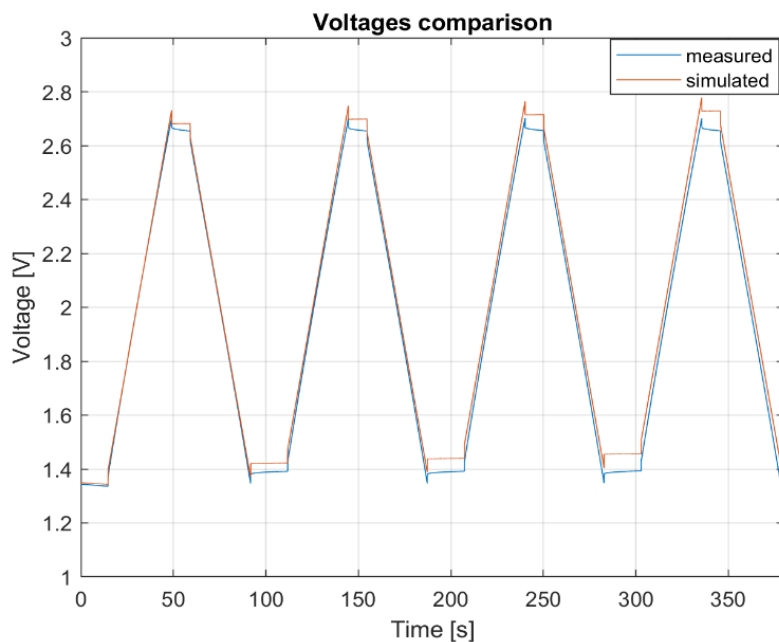
Figure 2.16 RC series model voltage comparison

What we can see in Figure 2.15 representing the voltage is that there is a clear mismatch between the two. We can therefore conclude that the model is too poor to provide a correct representation of the behavior of a supercapacitor. In fact, although at the beginning the trends are very close, the difference increases with time. Figure 2.16 shows is the absolute error calculated through the following equation.

$$E_{abs} = V_{simulated} - V_{measured} \qquad\qquad\qquad 2.2$$

The absolute error is shown in Figure 2.17
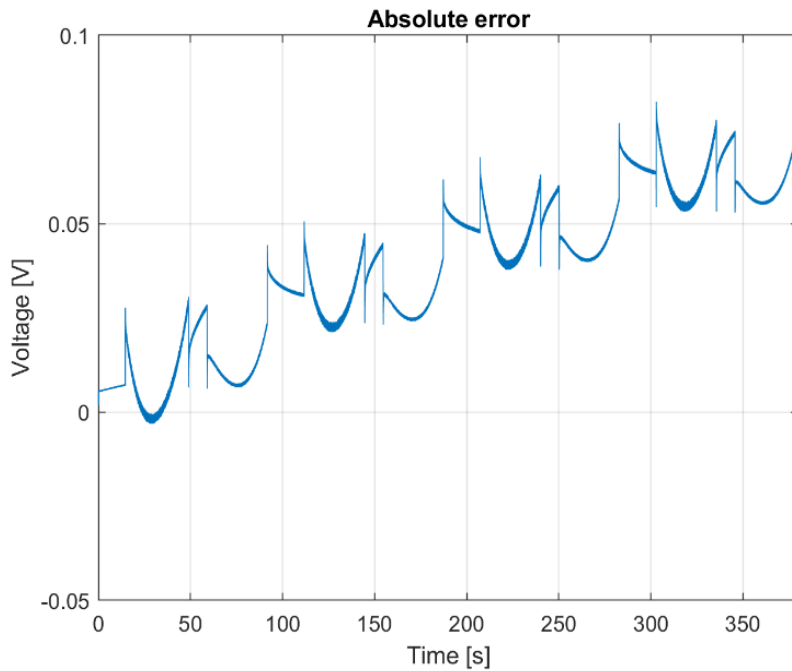
Figure 2.17 RC series model absolute error

We then move on to a more specific point of view looking at the relative percentage error. The model clearly cannot represent the component. Now the following equation is used to calculate the relative percentage error.

$$Er\% = \frac{V_{sim} - V_{meas}}{V_{meas}} \times 100 \qquad 2.5$$

Subsequently the data are displayed from the probabilistic point of view in Figure 2.19. The error is inserted into a fitting function, to find the probability density function of the error. In this way it is possible to see precisely the density for each error value, showing more clearly where the error is concentrated. For this model, note that the distribution range is quite wide: in fact, the error increases with time and
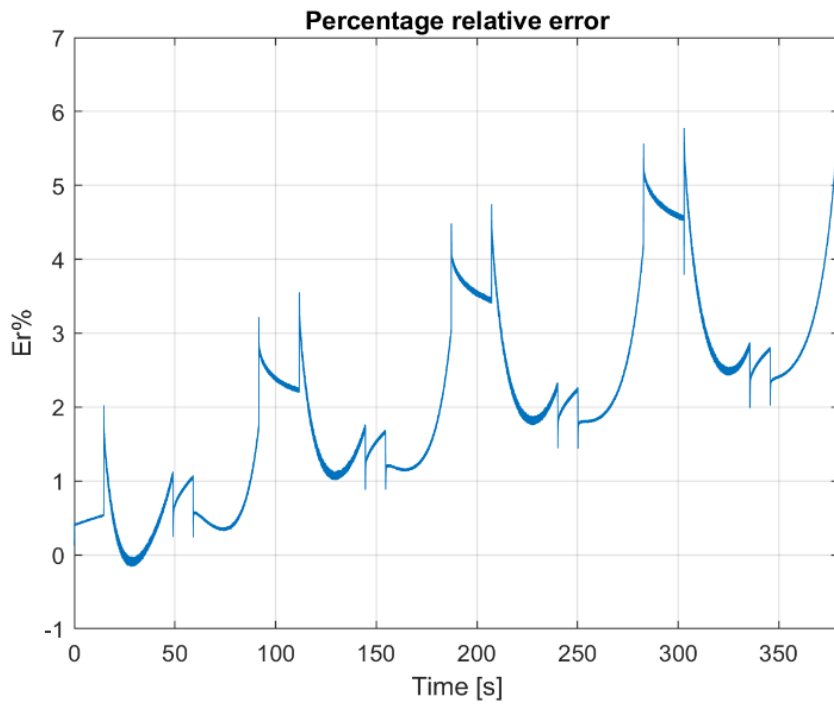
Figure 2.18 RC series model percentage relative error

this determines a wide range and a lower density value for each relative percentage error value.
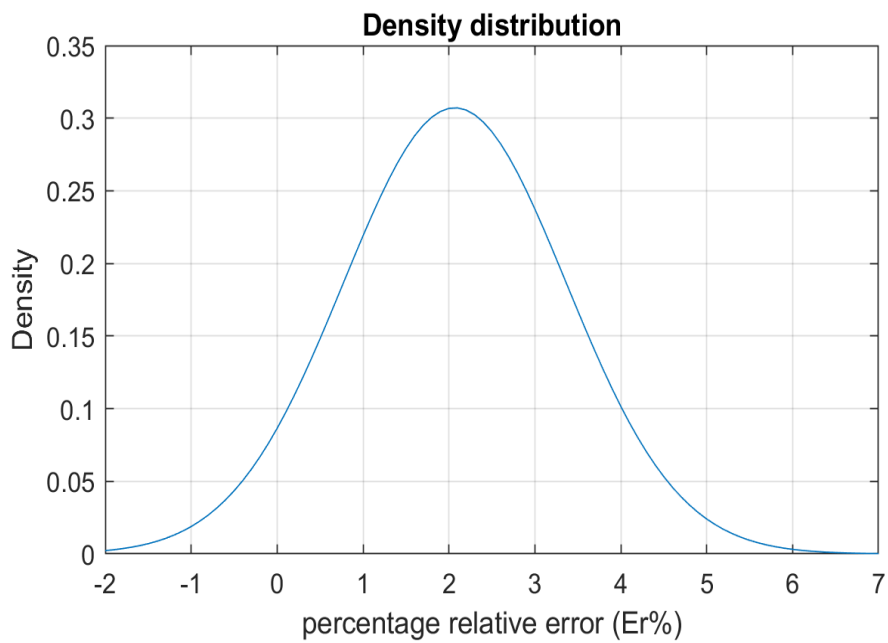
Figure 2.19 Percentage relative error density distribution

Parameter	Estimate	Standard Error
μ	2.06856	0.00210682
σ	1.29873	0.000148975

Table 2.4 Parameters of the distribution function of the RC series model

The next model analyzed is the Two-Branch model. For the reasons already explained, the entire analysis process will be carried out with the simplified Two-Branch model.
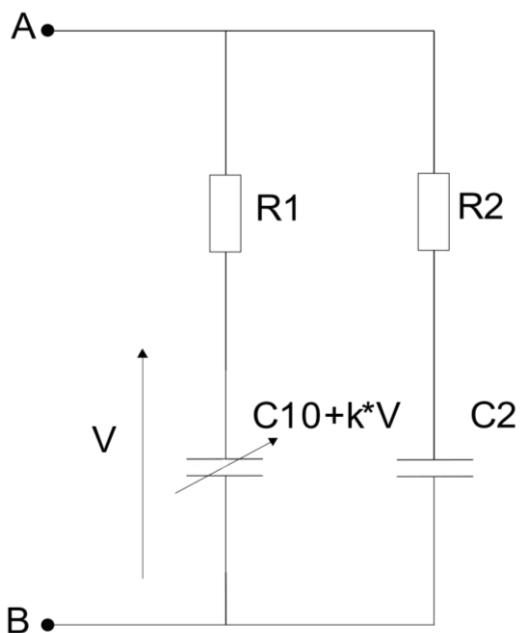
Figure 2.20 Two-Branch model

There are five parameters that will be estimated in the model. The model is not yet excessively complex, therefore, starting from not too random values, the estimation procedure does not take a long time.

Parameter	Value
C10	2968.96 F
R1	0.334e-3 Ω
k	121.129 F/V
C2	487.8 F
R2	0.4672 Ω

Table 2.5 Two-Branch model estimated parameters

We can see from the estimated values that R_1 is the parameter that represents what would be the series resistance of the component and C_{10} is the main capacitor of the model with a value really
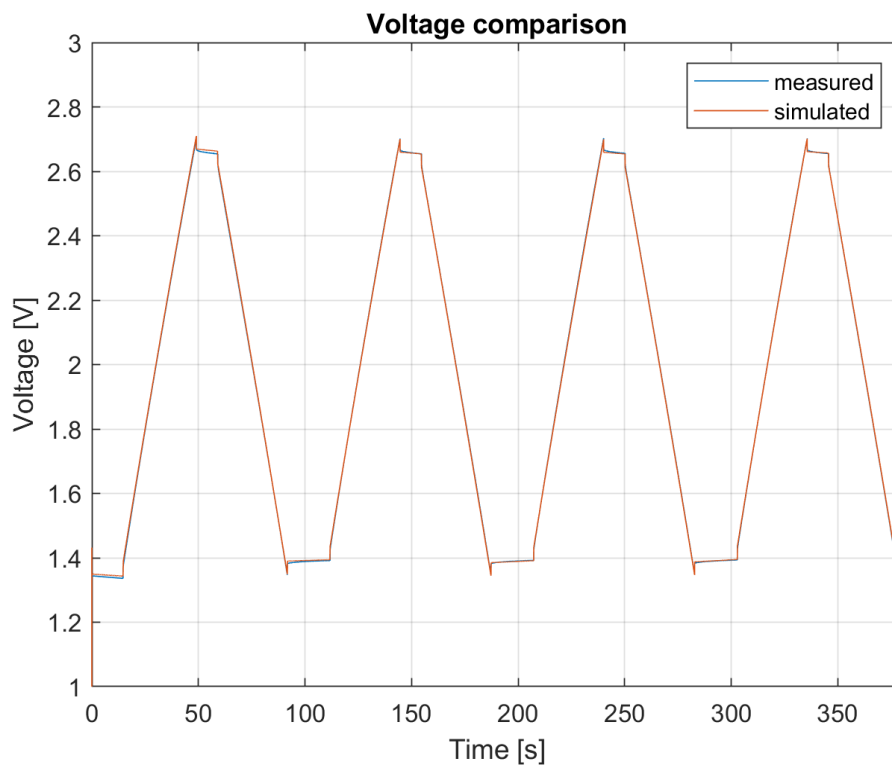
Figure 2.21 Two-Branch voltage comparison
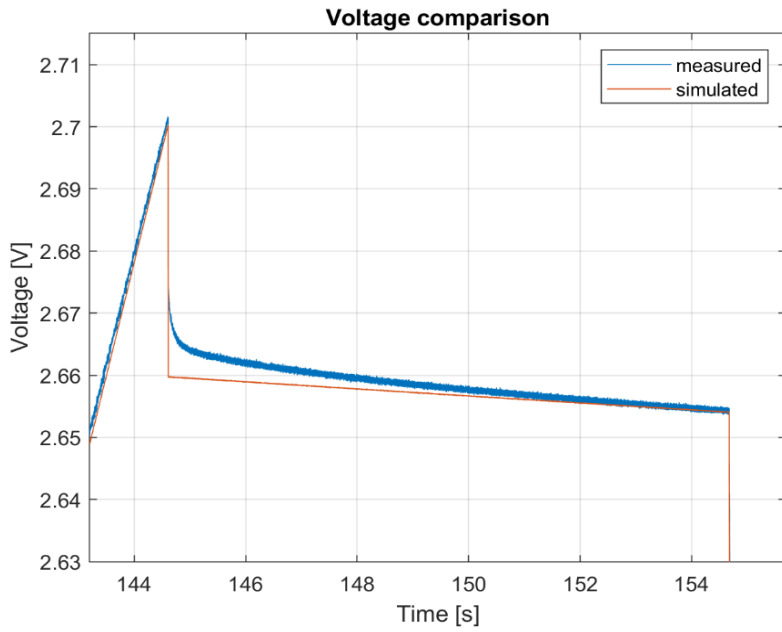
Figure 2.22 Second positive peak

close to what is declared by the manufacturer. It can be seen that the time constants of the two branches are different.
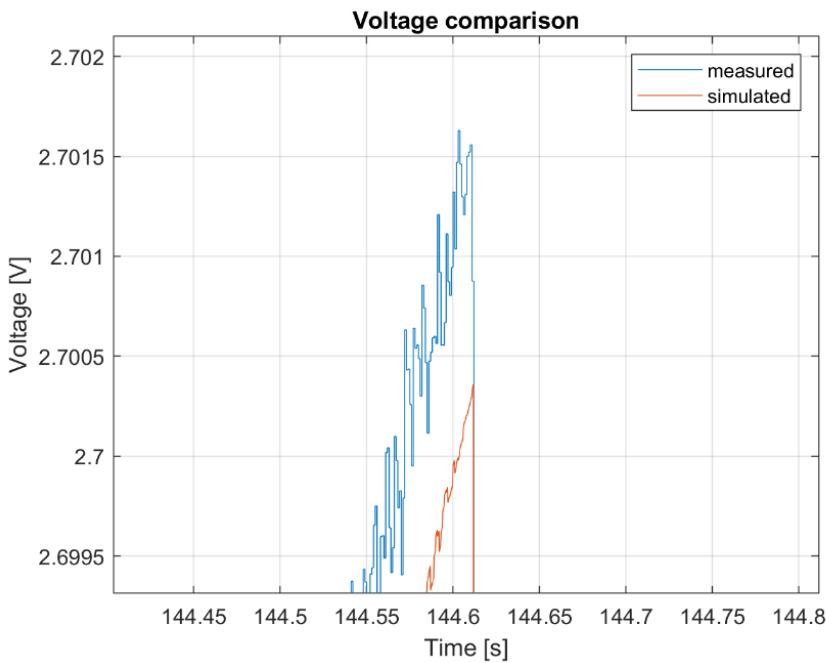
Figure 2.23 Peak of the second peak
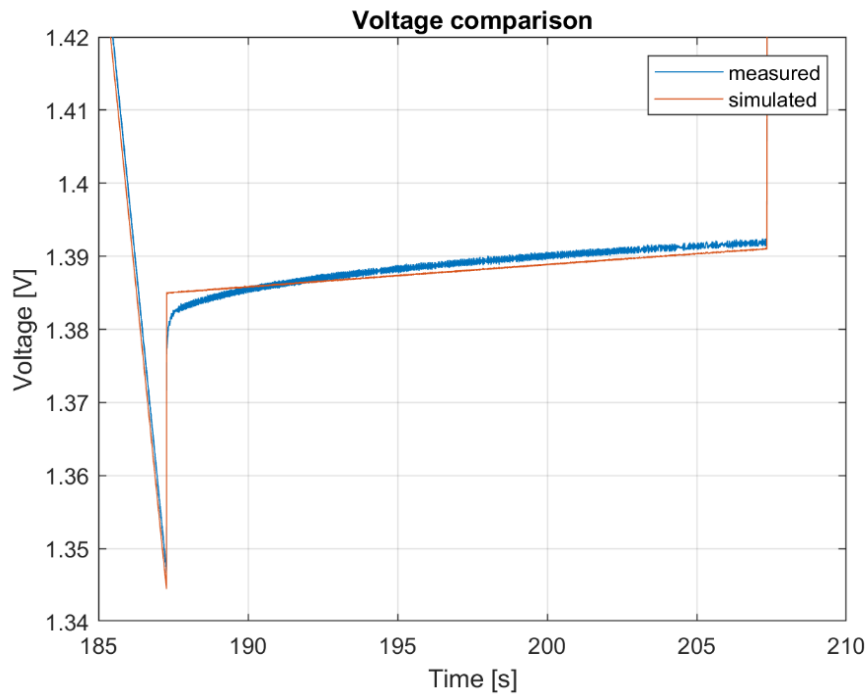
Figure 2.24 Second negative peak
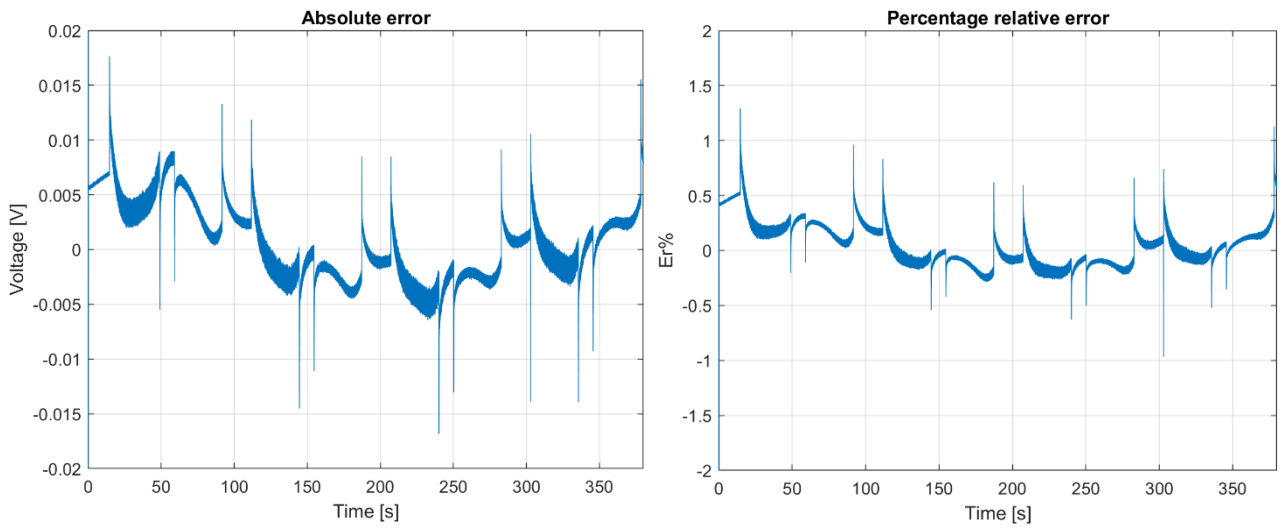
Figure 2.25 Two-Branch absolute error and percentage relative error

Looking at the voltage response of the model, it can be seen that it is close to the measured value.

Leaving aside the first cycle for the above-mentioned reasons, one can better observe the critical

points of the representation.
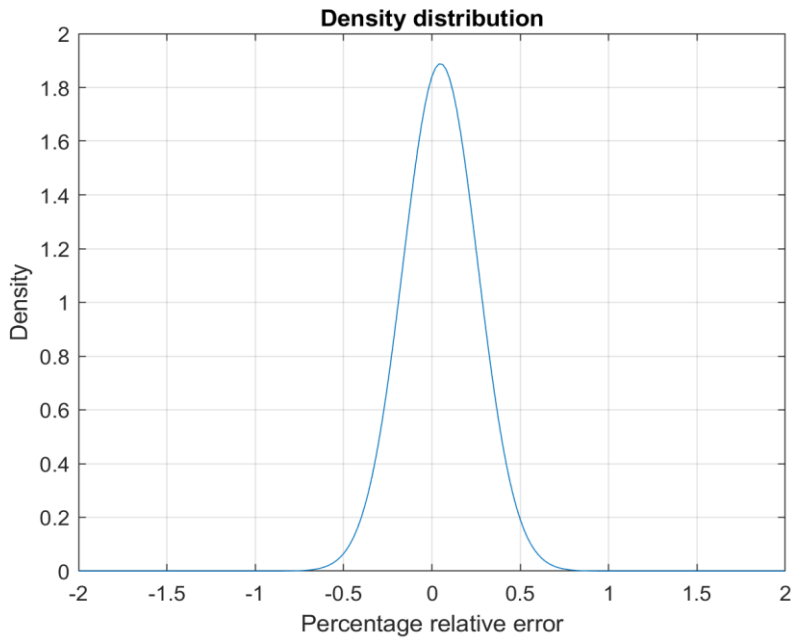
Figure 2.26 Two-Branch density distribution

 From Figure 2.26 it can be seen that the difference is minimal since the absolute error is around

0.005. To better see the accuracy of the model, after looking at the negative peak to see that there are

no big differences between positive and negative, the errors are shown. In fact, we see that the error

is minimal and acceptable. It is below 1% and has a periodical trend. This means that, in a longer test

period

Parameters	Estimate	Standard Error
μ	0.0479518	0.00017131
σ	0.211205	0.000121135

Table 2.6 Parameters of the Two-Branch relative error density distyribution

there would be the possibility that this error always remains within a certain range. Which does not happen for the RC model for example, where an error increasing with time is observed. What is interesting to see is that the error is around 0. But this can be seen better by the density distribution function, where the density for each error value is highlighted.

The next model that will be analyzed is the Zubieta model, which is very similar to the previous one.
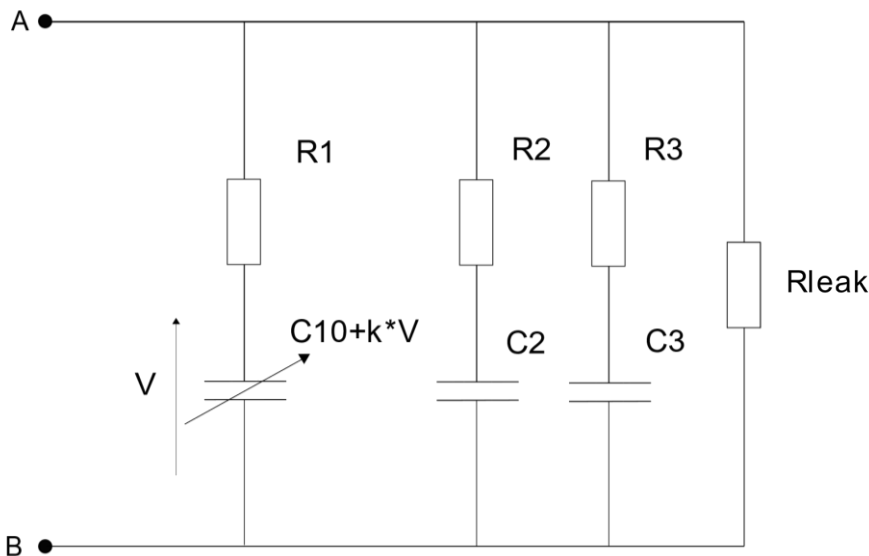
Figure 2.27 Zubieta model

Parameter	Value
C10	2934.7 F
R1	0.32232 mΩ
k	130.81
C2	76.841
R2	0.38065 Ω
C3	1518.8
R3	1.3284 Ω
Rleak	59436 Ω

Table 2.7 Estimated parameters of the Zubieta model

The value of the main storage component is 2937.7 F, and it is close to the declared value in the data sheet. The value of R1 is also close to the value of the equivalent series resistance.

In this case all parameters are estimated for a total of eight. Again, we have the main capacitor C10 and a factor k that multiplies the voltage across it. As can be seen, the time constants of each branch are different, and vary from the fraction of a second to tens of minutes, covering a period of about
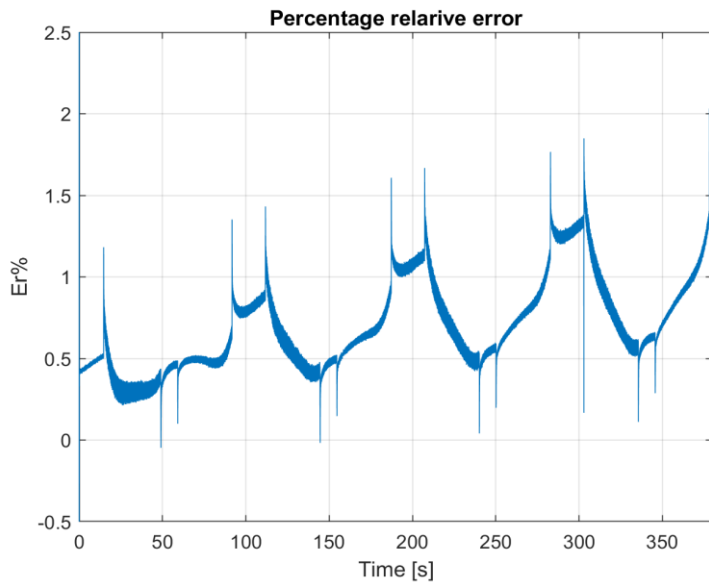
Figure 2.29 Percentage relative error of the Zubieta model

thirty minutes fairly evenly. The graph of the voltage across the model during its execution, however, the model accuracy is not better than the two-branch model. It can be seen that the error is
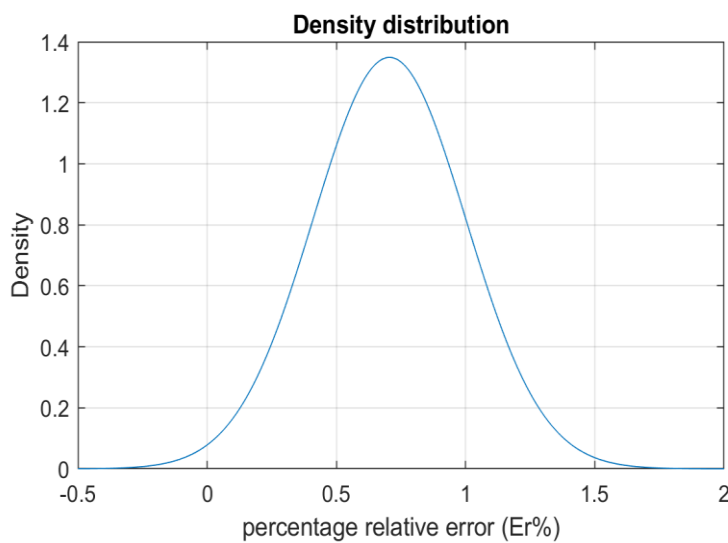
Figure 2.28 Density distribution of the percentage relative error of the Zubieta model

increasing. Error values are higher than the Two-Branch model although they are very similar. The

error distribution is not centered in zero: this means that on average the error is not zero.

Parameters	Estimate	Standard Error
μ	0.705316	0.000239882
σ	0.295746	0.000169622

Table 2.8 Parameters of the percentage relative error density distribution of the Zubieta model

The last model analyzed is the Series Model. This, due to its complexity, requires some precautions

in estimating the parameters. In the parameters estimation it results difficult to estimate many

parameters cause of the risk of find local minimums. To avoid this, some parameters are set to

reduce the number of estimated parameters. Particularly, to implement the model on

MATLAB/Simulink lookup tables are used.
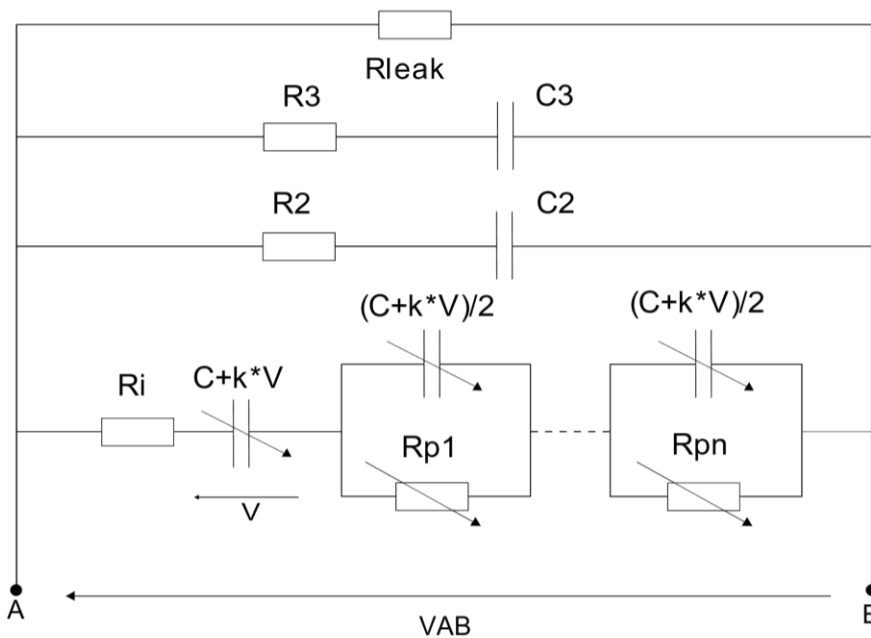
Figure 2.30 Series model

Parameter	Value
R2	55.9 mΩ
C2	95.11 F
R3	676 mΩ
C2	453.27 F
Rleak	63186 Ω
Rps	49799e-05 Ω
C+k*V	3250F
Ri	0.32232 mΩ

Table 2.9 Estimated parameters of the series model

The lookup-table receives as input a voltage value and two arrays: one with the voltage values and one with the resistance/capacitance value. The two arrays (Equation2.3/Equation2.5 and Equation2.6)are used to do an interpolation of the value of resistance/capacitance as function of the voltage. So, once have received the input voltage, the lookup-table block gives as output the value of the variable component at that voltage.

So, setting the values of the coefficients and estimating the reference values of the arrays (Rps, Cest) for which they will be multiplied, we arrive at the implementation of the whole model. Table 2.10 contains fixed values used for the interpolation. Table 2.9 is instead containing reference values (Rps, Cest), that have been estimated.

Resistance			Capacitance		
rp_1(0V)	rp_2(1.35V)	rp_3(2.7V)	cr_1(0V)	cr_2(1.35V)	cr_3(2.7V)
0.965	0.97	0.98	0.88	0.92	0.95

Table 2.10 Coefficients values for the construction of the lookup tables

$$Lookup-table_{resistor} = Rps \cdot [rp_1 \quad rp_2 \quad rp_3]$$ *2.3*

$$C_{est} = C + k \cdot V$$ *2.4*

$$Lookup-table_{capacitor} = C_{est} \cdot [cr_1 \quad cr_2 \quad cr_3]$$ *2.5*

$$V = [0 \quad 1.35 \quad 2.7]$$ *2.6*

The condition of the starting voltage is 1.35V for all models (Figure 2.34). Figure 2.31 shows the voltage response of the Series model.
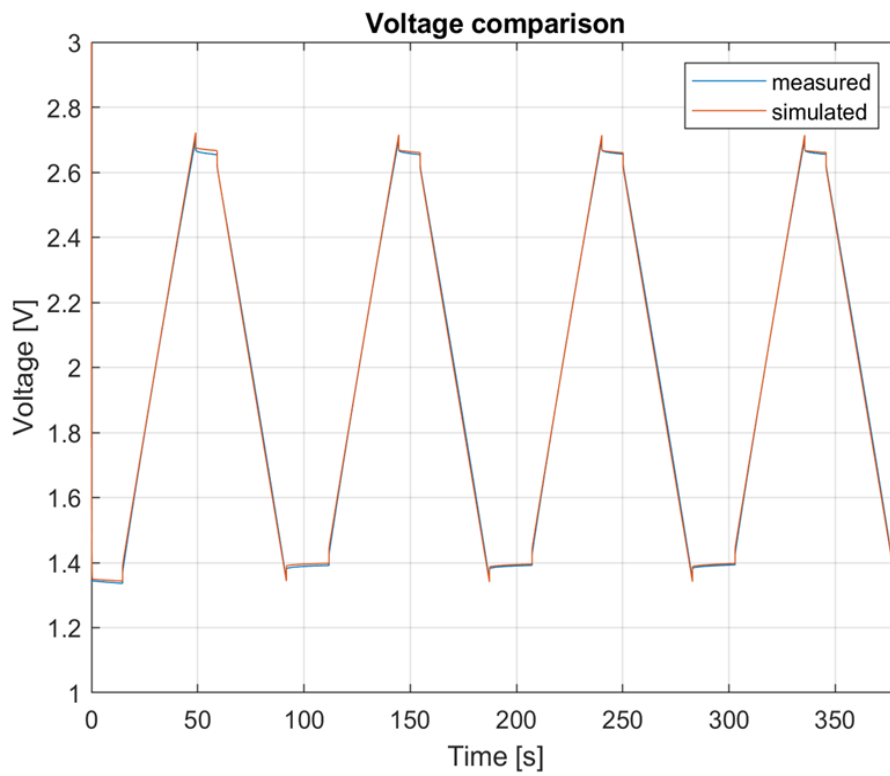
Figure 2.31 Voltage comparison with Series model output and experimental voltage

Note that at a glance the behavior seems satisfactory (see Figure 2.32), even giving observing the
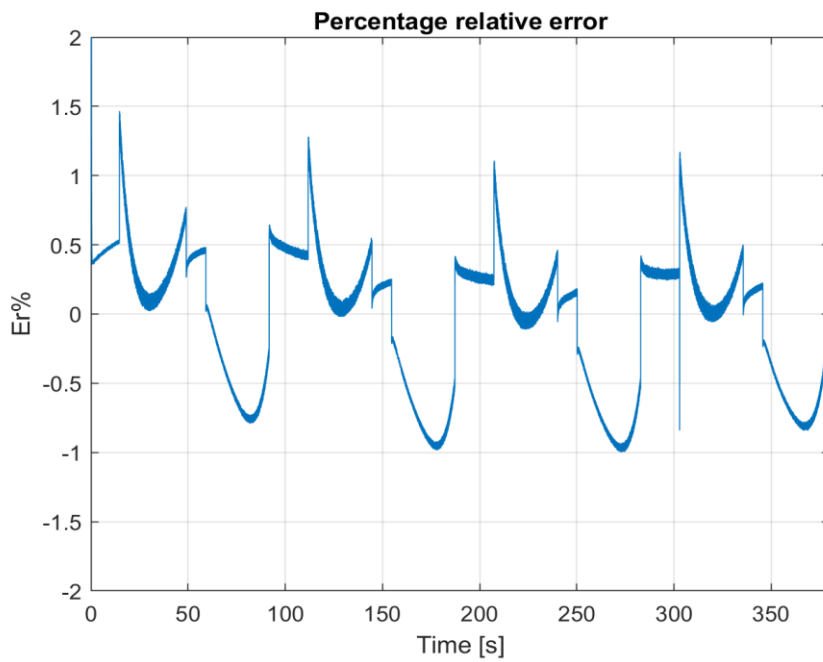
Figure 2.33 Percentage relative error of the series model

progress of the error it is. In fact, we can note that the error has a periodic trend, which means that

the model has good stability. The percentage relative error tends to remain around 0 as shown in

Figure 2.33, so it could be defined as stable.
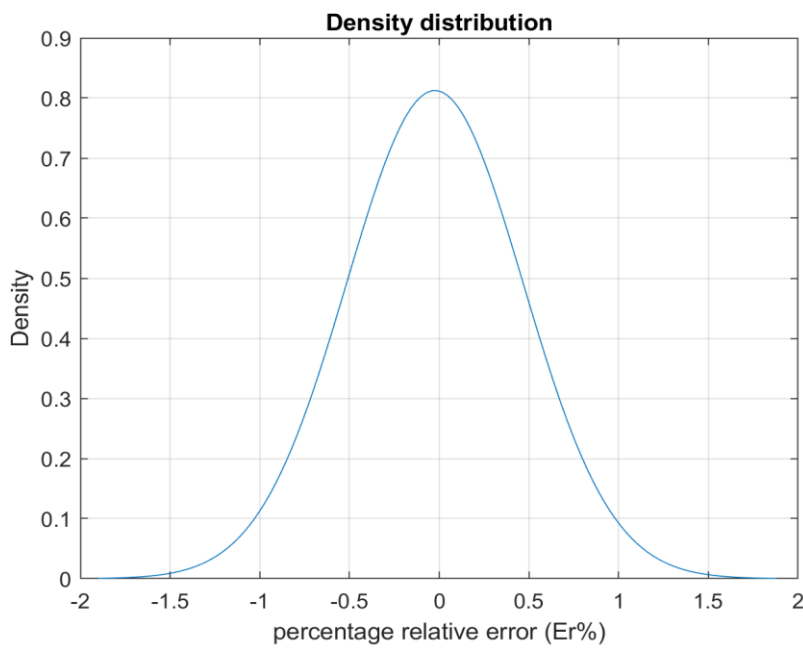
Figure 2.32 Density distribution of percentage relative error of the Series model

Parameter	Estimate	Standard Error
μ	-0.0240044	0.000796805
σ	0.490988	0.000563427

Table 2.11 Parameters of the density distribution of the percentage relative error of the Series model

To get an idea of which model is actually having the best performance it would be necessary to see their comparison. We start with the visualization of the voltages generated by each model. All the voltage responses are compared in Figure 2.34.They will be compared and analyzed in the critical points.
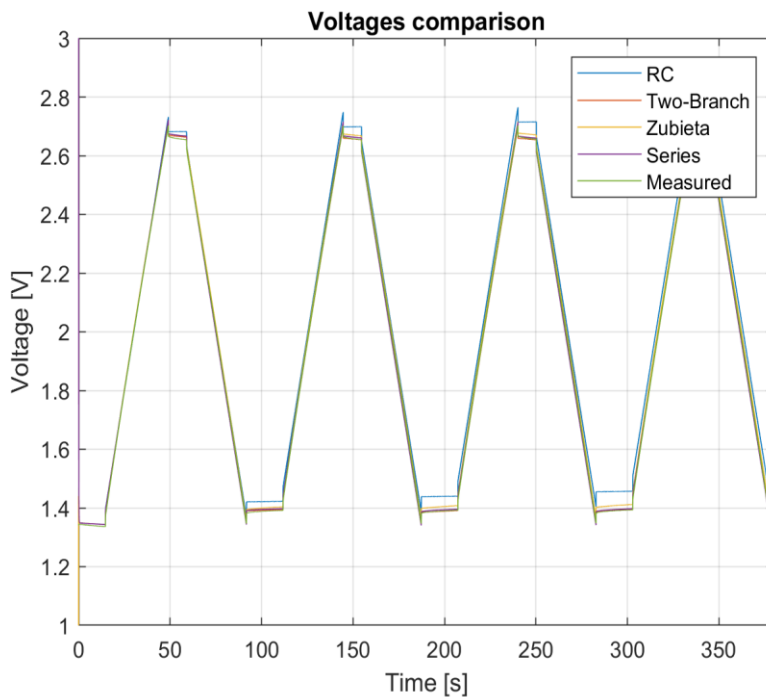
Figure 2.34 Voltages comparison of all the models

In addition, the voltage measured experimentally is also showed, as a reference. It is interesting to see closely at the behavior of the model in the critical points, which in this case are mainly the voltage peaks. In fact, in them there is the greatest mismatch for each model.

Starting from the first voltage peak we note that the voltages are all very close apart from the voltage

of the RC model which is already slightly higher. While Zubieta and Series models exhibit equal

voltage as shown in Figure 2.35. The Two-Branch model is the closest to the experimentally
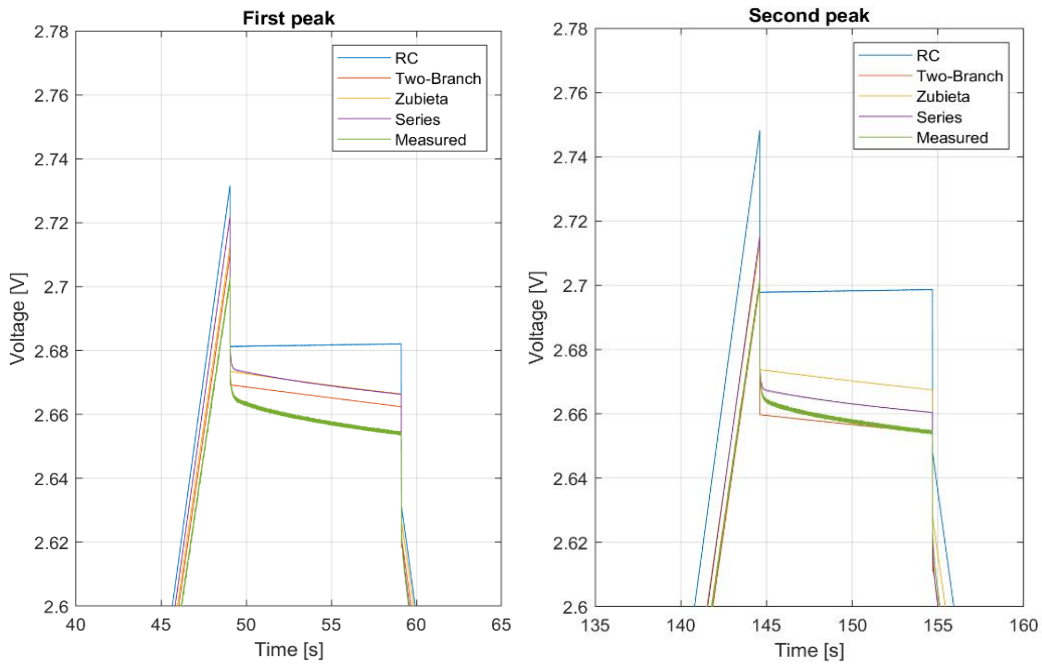
Figure 2.35 Detail of voltages in the first two peaks
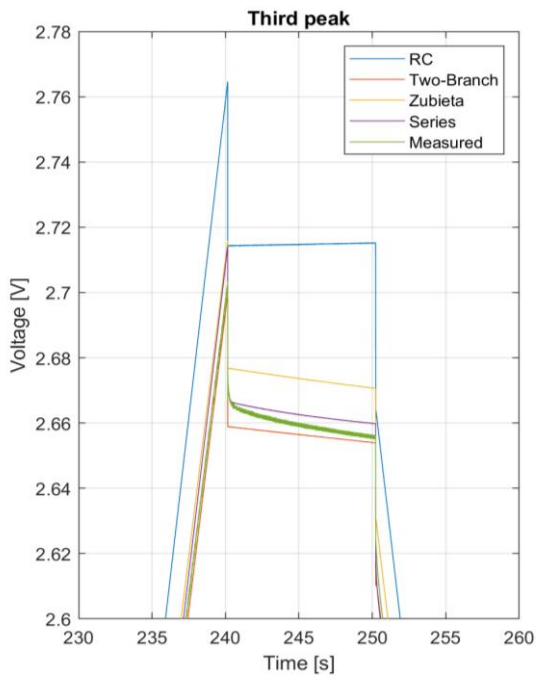
Figure 2.36 Detail of voltage in the third peak

measured voltage. Note that before the peak the voltage is rising when the voltage reaches 2.7V and therefore the injected current becomes zero, the series resistance contributes by slightly lowering the voltage value. It is important to note that the difference in amplitude that exists at this instant, i.e. after the voltage has been affected by the drop on the series resistance, is approximately the same as in the phase in which the voltage rose. So, this difference should not be associated with the abrupt variation because in fact it was present even before. In the second peak we can see how the voltage of the RC model moves away from the reference while that of the Two-Branch model goes slightly below the measured voltage. The Series and Two-Branch models are closest to the measured voltage, the Two-Branch model in particular. In the third peak in Figure 2.36 it is easy to see the voltage simulated by the RC model at a clearly unacceptable value while the Series and Two-Branch models remain close to the experimental value.

A comparison between the relative errors of the models is also shown in Figure 2.37 to compare their progress.
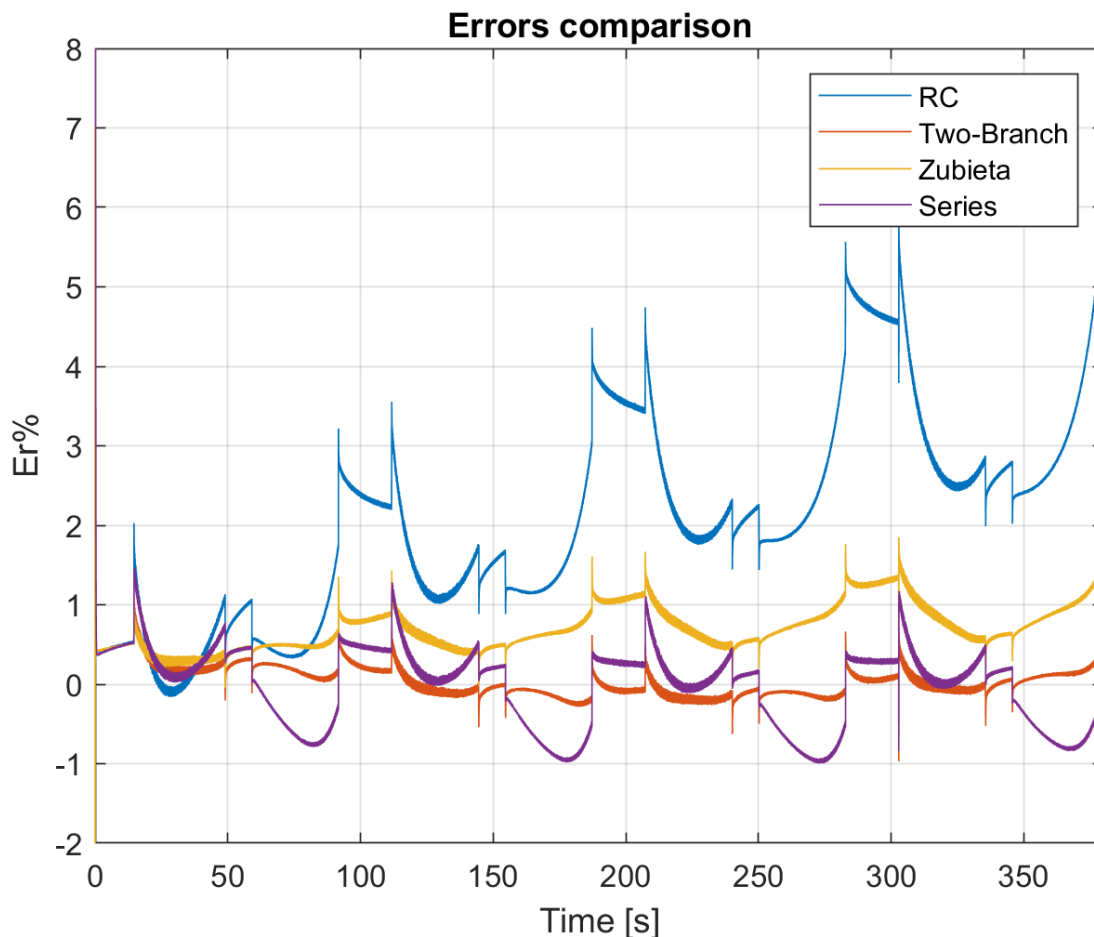
Figure 2.37 Relative error comparison of all the models

Figure 2.38 shows a comparison of the density distributions of all models.

The error of the RC model brings it shows that it is not suitable for representation. Its error grows over time and the density distribution with a wide range and low peak value highlight the inappropriate use. The trend of the error of the Zubieta model instead indicates that the trend is unstable as the error tends to increase. The density distribution is not very close to 0 but is still quite concentrated. However, the fact that the error increases makes it unsatisfactory. So, it is not good for
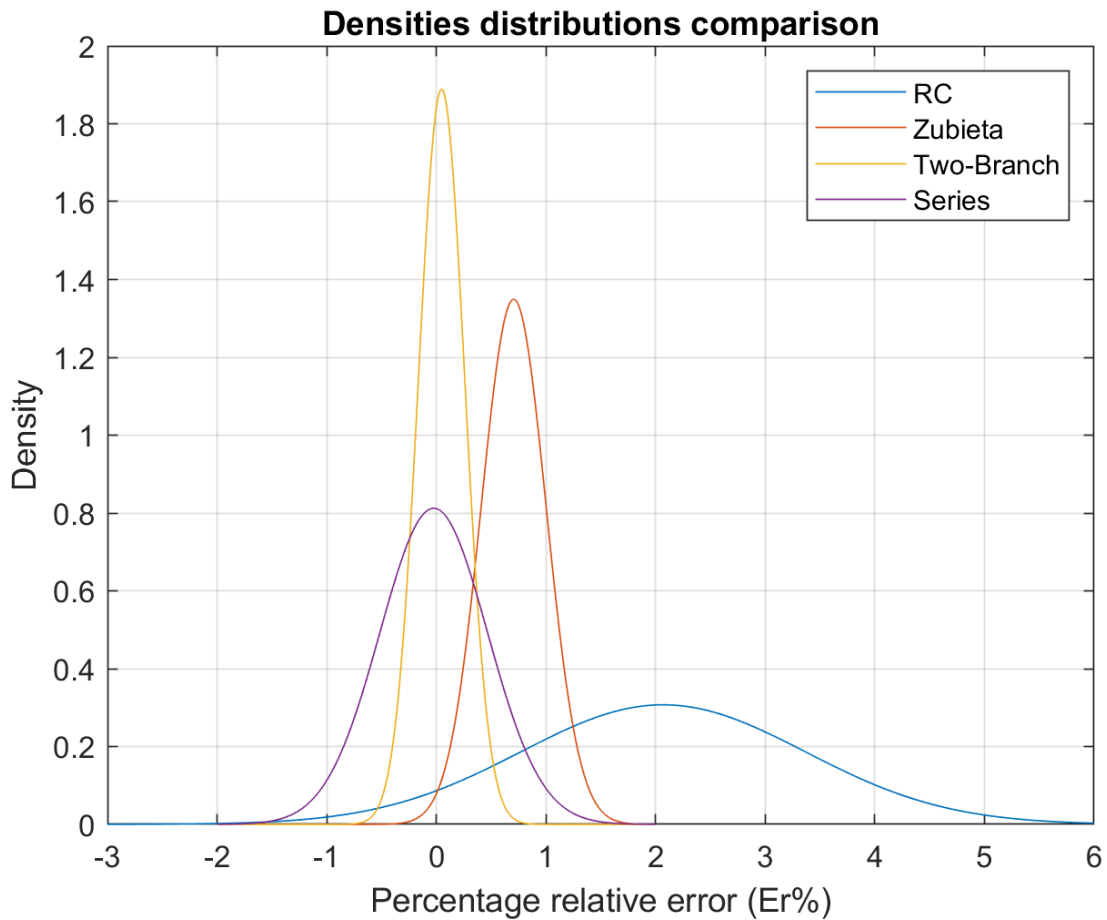
Figure 2.38 Density distributions comparison

the representation of the component. The remaining two models have already proved to be good

enough for representation. The trend of their error is therefore also satisfactory. In fact, they are both

periodic cycle after cycle remaining in a fairly small range and around 0. However, the range of the

Two-Branch model is smaller, and its peak density is therefore considered the best of the two. The

basis of the consideration is obviously the influence of the complexity factor of the model: in fact,

the Series model is more difficult to implement, with many parameters. Also, from this point of view

therefore the Two-Branch model would be preferable.

Model	Parameter	Estimate	Standard Error
RC series model	μ	2.06856	0.00210682
	σ	1.29873	0.000148975
Two-Branch model	μ	0.0479518	0.00017131
	σ	0.211205	0.000121135
Zubieta model	μ	0.705316	0.000239882
	σ	0.295746	0.000169622
Series model	μ	-0.0240044	0.000796805
	σ	0.490988	0.000563427

Table 2.12 Parameters of the density distributions of all the models

3 Chapter 3: Real-Time simulation of Supercapacitor

3.1 Real-Time simulation and its applications

In this chapter, the concept of real-time simulation is introduced, and a new tool to analysis and design of components and power systems is explained. In particular, we start with the introduction of DRTS (digital real-time simulation) as a tool for the representation of power systems in a real way, reproducing their behavior in real-time. The systems are first represented through particular software with user graphic interfaces and are then simulated in particular platforms. For real-time simulations time, in order to have a correct data acquisition it has to be

EXECUTION TIME (T_e) ≤ TIME STEP (T_s)

The execution time is the sum of time needed for measurement, computation and command. This sum has to be smaller than the set step time. Otherwise, an overrun will occur and an increase of the time step will be necessary. Overrun is when the time of these three parts exceeds the given simulation step. If this problem occurs, it is necessary to modify the simulation step time

Real-time simulations enable Hardware-in-the-Loop (HIL) testing, in which parts of the simulated system are replaced by physical components using input-output interfaces. Here the hardware under (HuT) test may be controllers that regulate switches or the connections and disconnections of some components. If controllers are tasted it is called CHIL (Control Hardware in the Loop). In these systems there are no real power flows and the whole system is modeled as something virtual that is inside the simulator.
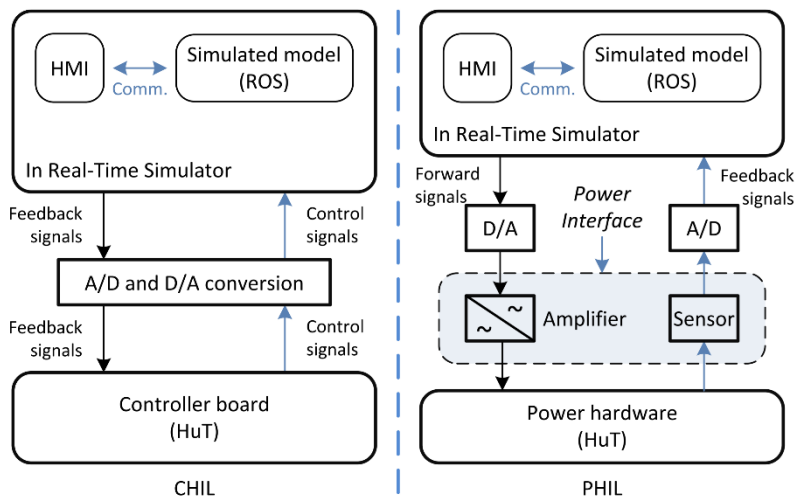
Figure 3.1 Controller Hardware-in-the-Loop (CHIL) and Power Hardware-in-the-Loop (PHIL).

[11]

When there is a real hardware under test, we talk of Power Hardware in the Loop (PHIL), as in Figure

3.1. In the PHIL there is a power interface that can both absorb and generate power, allowing bi-

directionally of the power flow. So, in PHIL it presents a power transfer to or from the Hardware

under Test (HuT). Both in CHIL and PHIL is present the human machine interface (HMI). There is a

simulated system part and an externally connected part. The power source can supply or generate

power. Then, the system is solved and the signals that are generated go to the HuT. First, they are

sent to an amplifier that supplies voltage or current to be applied to the HuT.

The first simulators were based on a digital signal processor. There was an expansion of general-

purpose processors because they were cheap, and their development cycle was fast. RTDS

Technologies Inc. launched the first digital real-time simulator on the market in 1991[11]. It has

combined analog and digital parts. The OPAL-RT Technologies Inc. simulator was introduced

around the year 2000. ARENE (from Électricitè de France), NEOTOMAC (from Siemens) were

introduced in the same years. OPAL-RT is the only one using MATLAB / Simulink as a simulation modeling tool.

A real-time simulator must be able to solve the model under 50µs, this in order to have a good accuracy of power system phenomena. If instead one needs analyze something faster like a microcontroller where there are higher frequencies, the time can be around 1µs or even 10ns. However, it can happen that there are very fast internal dynamics, but it is not necessary to use a very
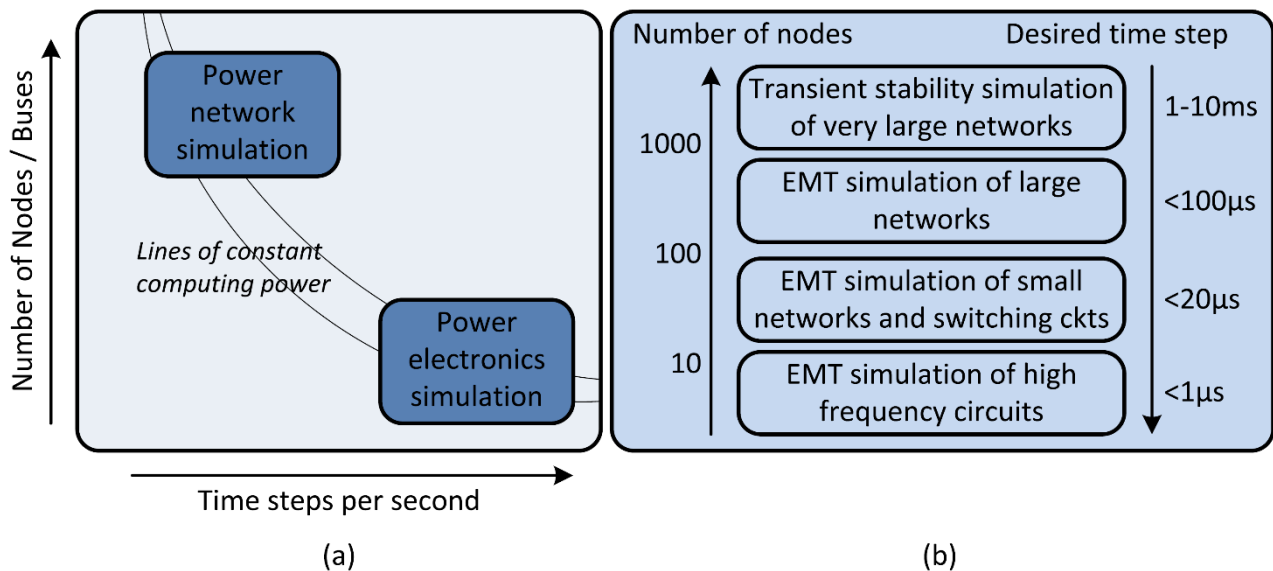
Figure 3.2 Capability requirements (a) and time-step requirements for different systems

small time-step. Figure 3.2 ([11]) shows the relationship between computing nodes and time-step requirements for different systems. The simulation of the power system simulation can be carried out with comparatively larger time-step, and for a constant computing power, it allows a larger system, whereas for power electronics simulation, smaller time-steps are necessary, resulting in a smaller system for the same computation power. It is possible to increase the calculation power of the simulator as the parallel operation unit, but a delay for communication is added. Communication is

optimized by exploiting the properties of the transmission lines separate the network subsystems with an adequate length, consistent with the simulation steps.

Most simulators have the following characteristics:

- multiple processors working in parallel that form the platform where the real-time simulation is performed

- an external computer on which the model previously created offline, built online, uploaded and executed (using the same computer to monitor the simulation)

- input-output terminals for the hardware interface

- a communication network in case the model is divided into several subsystems
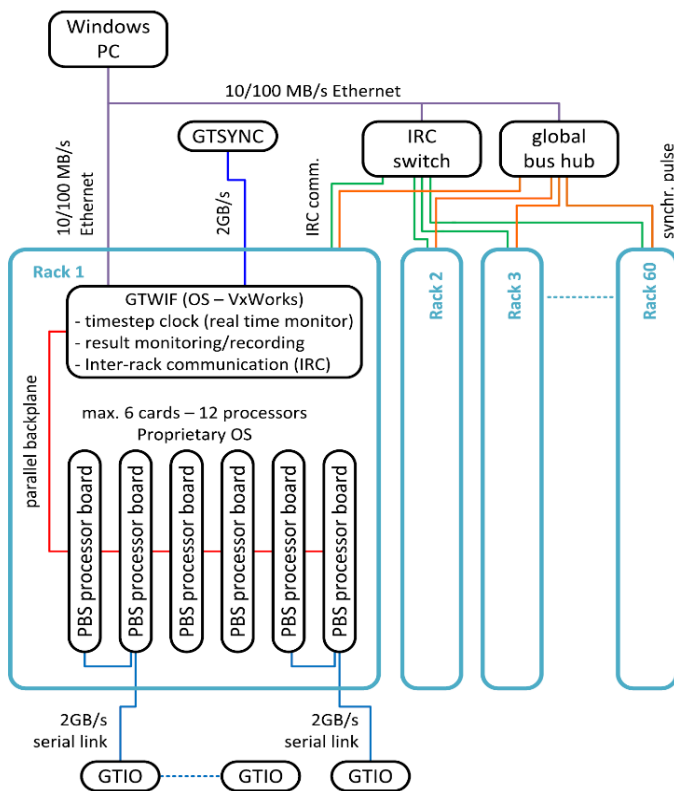
Figure 3.3 Example of hardware type A

An example of hardware of type A is shown in Figure 3.3.

Now we move on to a hardware description starting with the description of type A [11]. This is made up of various units called racks that contain various processor boards. Each processor board contains two processors that work in parallel. They make up the main calculation engine. Each rack is therefore made up of twelve processors or six boards. The maximum number of nodes of the power network that can be simulated is 72. There is a network solution for each processor. Each simulator also contains a workstation network interface: this allows communication and synchronization with real-time operation of the components. Through the use of some cards it is possible to switch to a synchronization that can also facilitate the connection with the outside. By combining processors, more effective results were also obtained.
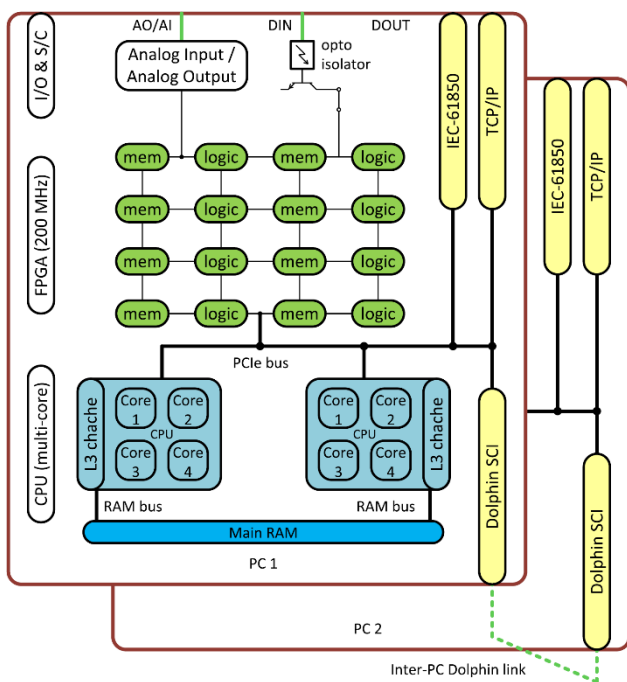
Figure 3.4 Hardware architecture of eMEGASIM real-time simulator

The type B simulators (architecture shown in Figure 3.4 [11]) have undergone rapid development of communication techniques and protocols for sharing. All this thanks to the rapid development of network and communication technologies. Type B is the multi-CPU simulator. This can be extended to multicore with each core modeling a subsystem. The shows how the various hardware components

are connected. There are reconfigurable FPGA (field programmable gate array). The input-output signals are conditioned by these FPGAs. This type of simulator, which can also use different toolboxes, personalizes the system by orienting itself towards the integration of FPGA components, graphics processing unit (GPUs) or in any case sets of hardware components.

The type B is of interest for this work. Particularly Figure 3.4 shows the structure of the simulated used in this analysis. In fact, eMEGASIM is the software used. It is compatible with Simulink and Simscape Power Systems MATLAB tools.

From the point of view of software, simulators can generally request two categories of software: operating system or application software. In general, the simulators work both on Windows and on Linux operating system, however, if necessary, in some cases particular operating systems may be necessary. Generally, in these cases the systems are supplied together with the hardware. Software applications in general can have particular interfaces and system configuration platforms in which the model can be adapted so that it is correctly read by the simulator and executed.

As for the interface and communication, type A connections are available for all racks to facilitate communication. In addition, fiber optic connections are used. In the event that there are more than seven racks, an inter rack communication is carried out with a point-to-point methodology. All this using Ethernet. On the other hand, for types B, thanks to the rapid technological advancement, there are various communication techniques and protocols used for the transfer of information. These include inter CPU communication signal wire, InfiniBand and others.

The modeling tools for type A simulators are available GUI libraries as an integral part that allow the construction of power system models with the necessary controls and protections. As far as the time-step is concerned, there is a time between 1-4 microseconds, therefore small, for the subsystems but

which can be easily adapted to interfaces with models operating at 50 microseconds times through various types of interfaces. The methodology followed for the interfaces is similar to that for the division of the various racks. If you want to interface systems with further lower time-steps, you can do it thanks to an FPGA modeling that allows a modeling at the desired frequency and an adaptation in every range. For type B variants there are MATLAB / Simulink type development environments. If you want to write in a high-level language such as C ++ or FORTRAN, they can still be inserted in the MATLAB/Simulink interface. There are also expansion types of the MATLAB / Simulink environment. The methodology for solving the model equations in two type of simulators varies. For type A, the whole circuit and every component is discretized. Then it proceeds with a matrix subdivision in which the impedance matrix is subdivided as the various impedance sequence components. For type B, an admissions matrix resolution system is used. In this case, models are built on particular platforms with solution algorithms such as backward Euler available in MATLAB / Simulink for discrete solutions. However, these solvers are not suitable for this type of simulation as the solution time can vary. ARTEMIS-SSN is a solver that provides a good analysis of the switching events and a fairly fast resolution. The I/O is generally located inside the simulator and then connected through an optical fiber. However, it can also be placed under wire and connected by cable. For type B, multichannel modules may be present. Having scalable terminals, they have a good resolution and a very precise timing. Outside the market there are some simulators that are developed for specific purposes. One of these was developed in the University of South Carolina. A new process has been developed in Aachen University in Germany [12].

Applications of real-time simulations were first oriented towards transmission lines, the control of protection systems and the validation of controls. Then as time went on, analyzes began to be required for more difficult components such as synchronous machines. In fact, their control, their

implementation, were something more complicated. Today, real-time simulations participate in the analysis of distribution networks due to the presence of smart grids and microgrids. In addition, there is designed electronic power converters which have a much more complex implementation. In fact, they have a much higher operating frequency and a huge number of inputs / outputs. There are therefore various applications for these simulators that concern product design as well as prototyping and testing of the same component.
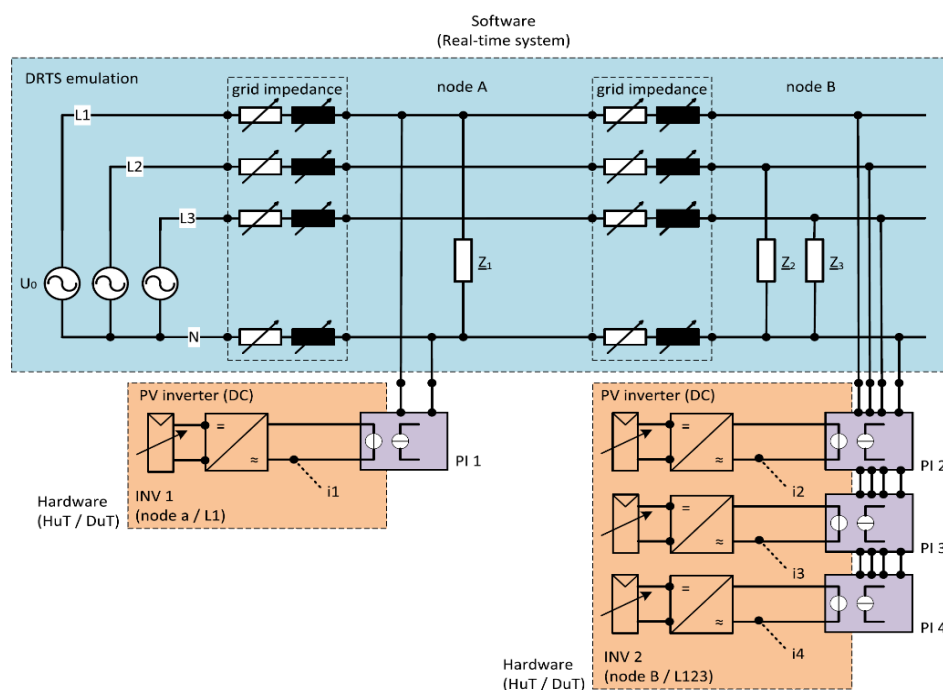
Figure 3.5 Inverter power analysis inside a photovoltaic system with power hardware in the loop

Real-time supercapacitor simulation model applications are required prior to the PHIL test of supercapacitors, for the PHIL test of DC-DC converters for supercapacitor energy storage systems and for the CHIL test of controllers for supercapacitor energy storage systems.

The simulation models are implemented in RT-LAB. The models are simulated on Opal-RT's OP4510 real-time simulator.

3.2 Real Time implementation and setup

In this work, the models were implemented in MATLAB/Simulink and subsequently adapted for the RT-Lab platform. The model blocks are grouped and divided into sub-systems, as requires by RT-Lab. In particular, a splitting by groups was performed. Figure 3.6 is an example of blocks splitting. In this example is shown how the computational blocks are grouped together in the computation subsystem, while all those input or display blocks are inserted in the GUI subsystem. The two subsystems are linked as in Figure 3.7.
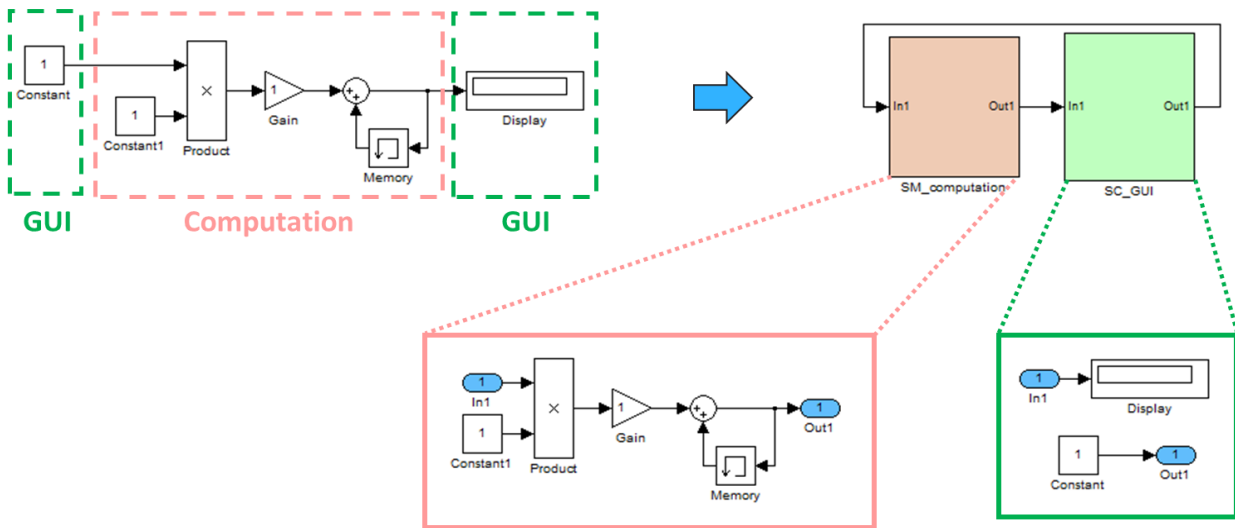
Figure 3.6 Example of blocks division for RT-Lab. Picture courtesy of: Opal-RT Technologies

The computation block is executed in a CPU core of the real-time target. The GUI subsystem will be shown on the host PC. The data of the two subsystems are executed asynchronously.
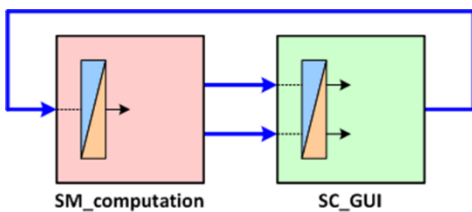
Figure 3.7 Example of Computation and GUI blocks. Picture courtesy of: Opal-RT Technologies

It is possible to create multiple computation blocks which would then be executed synchronously in two CPU cores, but this is not required for our case. 'OpComm' blocks will be inserted in both the Computation and GUI blocks, which will have the function of receiving the signals from the other real-time subsystems.
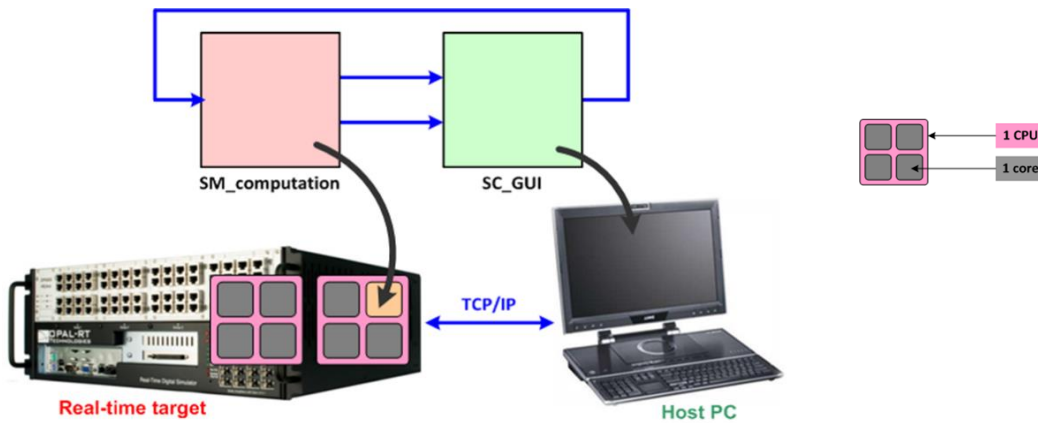
Figure 3.8 Grouping into subsystems. Picture courtesy of: Opal-RT Technologies

The model must first be run offline to verify its effective operation. Once it can be done offline, it is possible to start building the model with RT-Lab. When the project has been created in RT-Lab and
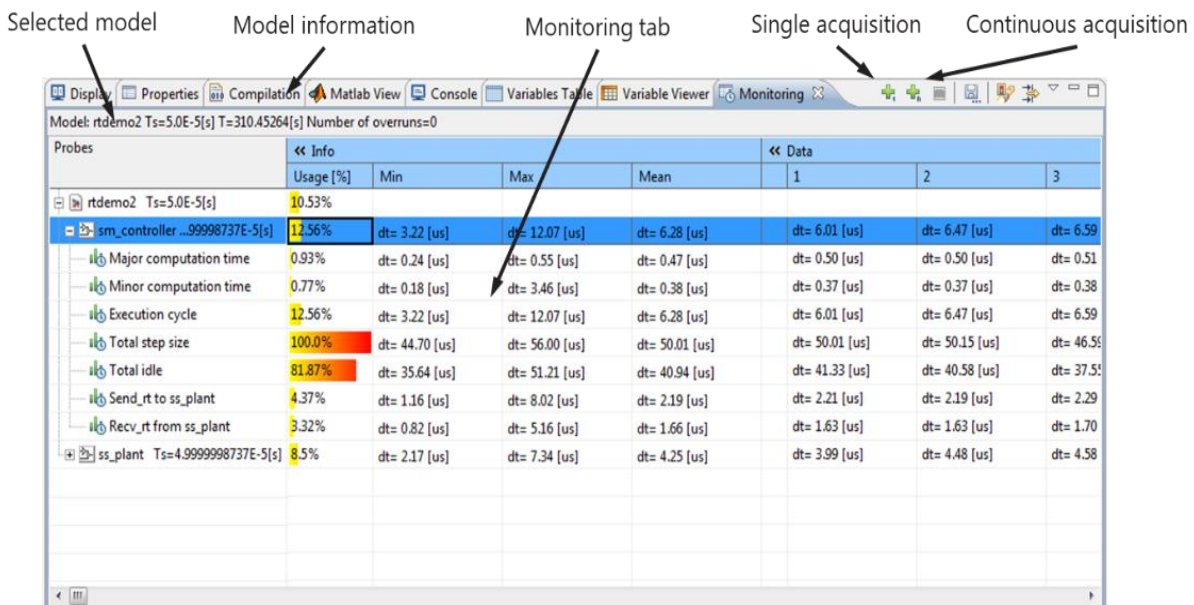
Figure 3.9 Monitor window. Picture courtesy of: Opal-RT Technologies

the model has been loaded, the program will create a C code. At the end of the procedure has been

completed, the code can be created, which can obviously be longer or shorter depending on the model, there will be loading on the platform and finally the execution. Once the model is run it is possible to monitor it. For each model, a fixed step-size and time must be specified (in this case 5e-05).

For monitoring the real-time execution of the model, RT-LAB extracts 100 consecutive simulation time steps and calculated average and maximum model execution time within these 100 time-steps. In fact, it may turn out that the time-step is not adequate, and this leads to an incorrect acquisition of values. In particular, what is called an overrun occurs. In practice, a time is set for the system within which measurement, computation and command must take place as shown in Figure 3.10.
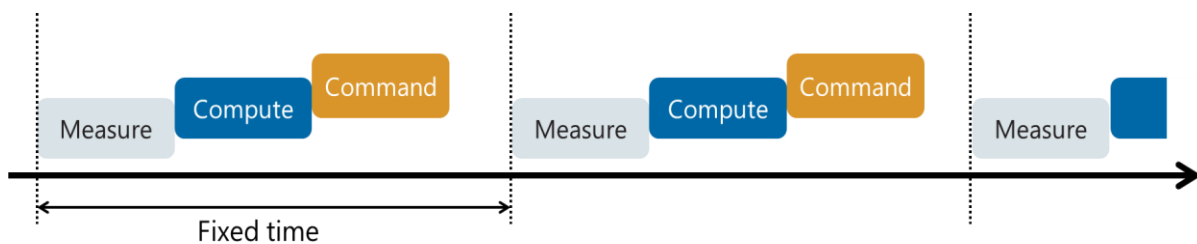
Figure 3.10 Correct time step. Picture courtesy of: Opal-RT Technologies

Overrun is when the time of these three parts exceeds the given simulation step. If this problem occurs (as shown in Figure 3.11), it is necessary to modify the simulation step time.
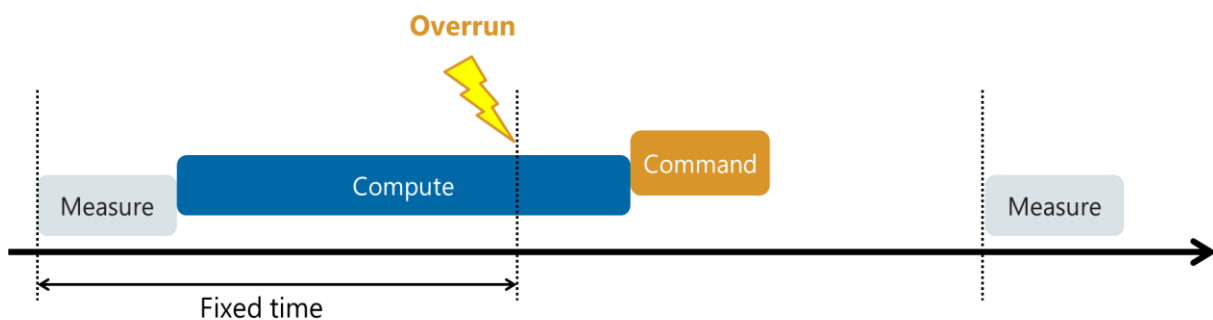
Figure 3.11 Overrun occurring. Picture courtesy of: Opal-RT Technologies

The implementation of the model for the RT-Lab platform is shown in Figure 3.12.
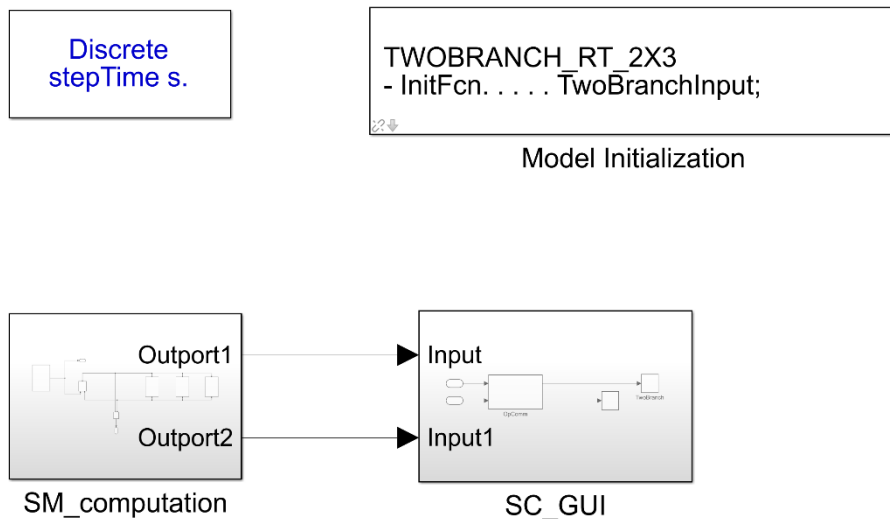
Figure 3.12 Two-Branch model implementation for the RT-Lab platform

The implementation is done grouping blocks in subsystems. Before running the model on the platform is necessary to set both a discrete simulation type and the step time. In this case, the starting step time is 5e-05 seconds for every model. In the Model Initialization block are given all the input parameters of the model. So, once parameters have been estimated, they are given to the model as input in this way. The Model Initialization block receives as input the 'file.m' containing all parameters. Figure 3.13 shows a computation block. It is possible to see that in this example three parallel branches are analyzed.
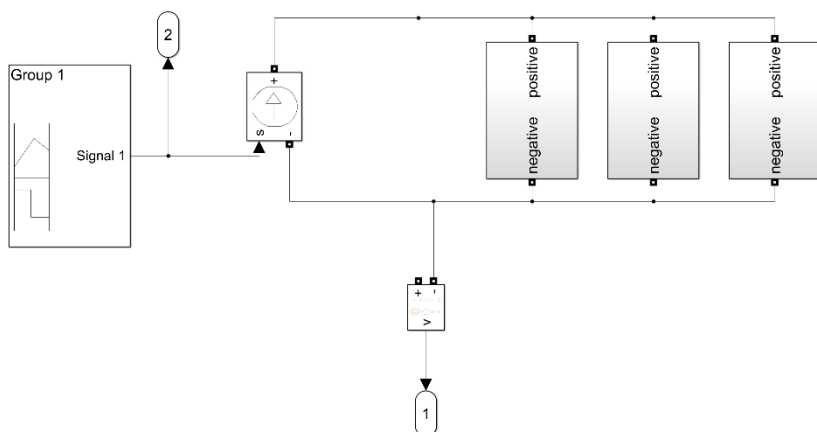
Figure 3.13 Example of the computation block of the Two-Branch model with three parallel branches with two series supercapacitor models each one

The simulations are performed on Opal-RT's OP4510 real-time simulation.

Here are the data of the used hardware.

OP4510

- Compact and powerful 2U real-time target with QuadCore processor @3.3 GHz

- Real-time operating system: Linux REDHAT

- Xilinx KINTEX-7 FPGA

- Total of 4 I/O boards

    - 16 Ain, 16 Aout, 32 Dout and 32 Din

- Rear DB37 connectors

- 4 optional 5-Gbps SFP optical interfaces

- Synchronization connectors

Figure 3.14 OP4510. Picture courtesy of: Opal-RT Technologies

3.3 Real-Time Simulation of a Single cell

Each model is implemented in MATLAB/Simulink is the representation of a supercapacitor cell. In RT-LAB, 100 simulation steps are analyzed and minimum, maximum and the mean of the model execution time are compared with each other. Remember that each model will have different execution times due to its structure and complexity.

	Model execution in real-time simulation			Model error (compared to experiments)	
Model	Min [μs]	Max [μs]	Mean [μs]	μ [%]	σ [%]
RC	0.47	0.54	0.49	2.06856	1.29873
Two-Branch	0.49	0.58	0.50	0,31608	0,18905
Zubieta	0.48	0.62	0.52	0.70531	0.29574
Series	0.50	19.06	1.44	0.80347	2.76186

Table 3.1 Real-time model execution time for single cells of supercapacitor models

Execution times are shown in the table above. Note that the table is made up of three columns indicating minimum, maximum and average time. For real-time simulation the maximum execution time is the most important parameter, as a single overrun can lead to inaccurate results. Starting from the RC model, the model execution time is very much below 1μs, this model is a very low computation time for real-time simulations. The Two-Branch and Zubieta models also have a good run time, slightly higher than the RC model but still abundantly below 1μs. As for the Series model, it is possible to note that the maximum time is much higher than that of the other models. This model is the most complex with the largest number of parameters, therefore the execution time must be higher. But what influences this value is mainly the fact that look-up tables and interpolation are present within the model. In fact, the presence of lookup tables that require an internal process to the

model greatly increase the execution time. As you can see, the average time is not excessively high considering that the maximum one is about 40 times the minimum one. This means that the maximum occurs not very often (only when interpolation is needed) which does not allow an excessive increase in the average execution time. So, summing up the general behavior we see that the models have execution times in line with expectations and coincide with the results of the offline times. Particular attention should be paid to the Series model which circuit is more complex. All models where simulated with a 50 microseconds simulation steps, as the models will need to be added to a power system model later on.

Simulation step time ≥ Maximum model execution time

3.4 Real-Time Simulation of Supercapacitors Stacks

In practice supercapacitor cells are used in stacks. However, cells can behave differently in reality. In particular, it is possible to see differences after a number of deep discharge/charge cycles. This difference leads to the need to analyze the results with multiple cells. Such models are required testing stacks management systems. To simulate the possible combinations, several tests were carried out. Several cells have been inserted in series and several branches in parallel. Then a combination of the two by inserting cells in series and in parallel. Table 3.2 shows the results of the RC series model.

Number of parallel branches		m / M / mean (series = 1)	m / M / mean (series = 2)	m / M / mean (series = 3)	m / M / mean (series = 6)	m / M / mean (series = 12)	m / M / mean (series = 24)
12	m	0.53	0.93	1.57	4.63	20.8	**88.92**
	M	0.64	1.06	1.72	4.91	25.6	**89.16**
	mean	0.56	0.96	1.62	4.67	21.1	**89.09**
6	m	0.48	0.56	0.79	1.59	4.62	20.85
	M	0.57	0.67	0.88	1.75	4.97	21.17
	mean	0.5	0.6	0.82	1.64	4.89	21.06
3	m	0.51	0.49	0.51	0.72	1.65	4.56
	M	0.64	0.58	0.64	0.79	1.73	4.91
	mean	0.54	0.5	0.53	0.74	1.63	4.65
2	m	0.46	0.47	0.49	0.54	0.88	2.33
	M	0.57	0.57	0.6	0.65	0.99	2.41
	mean	0.48	0.5	0.52	0.57	0.92	2.36
1	m	0.47	0.47	0.49	0.48	0.56	0.92
	M	0.54	0.56	0.59	0.58	0.66	1.02
	mean	0.49	0.5	0.52	0.51	0.59	0.94
Number of cells in series		1	2	3	6	12	24

Table 3.2 The model execution times for supercapacitors stacks using the RC series model

▮ 10e-5 stepTime	▮ 50e-5 stepTime	▮ 100e-5 stepTime	▮ 300e-5 stepTime
▮ 500e-5 stepTime	▯ 1000e-5 stepTime		
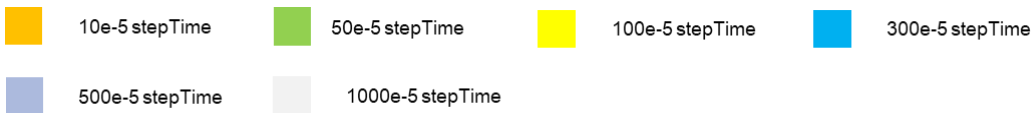
In the following table, the maximum model execution time is showed for different number of cells in series and parallel branches. Where the model could be simulated with simulation steps of under 50

microseconds, the table cell is showed in green. Otherwise, the cell in yellow, indicating a large model simulation step is required.

Model execution time (microsecond)

Number of parallel branches	1	2	3	6	12	24
12	0.64	1.06	1.72	4.91	25.6	89.16
6	0.57	0.67	0.88	1.75	4.97	21.17
3	0.64	0.58	0.64	0.79	1.73	4.91
2	0.57	0.57	0.60	0.65	0.99	2.41
1	0.54	0.56	0.59	0.58	0.66	1.02

Number of cells in series
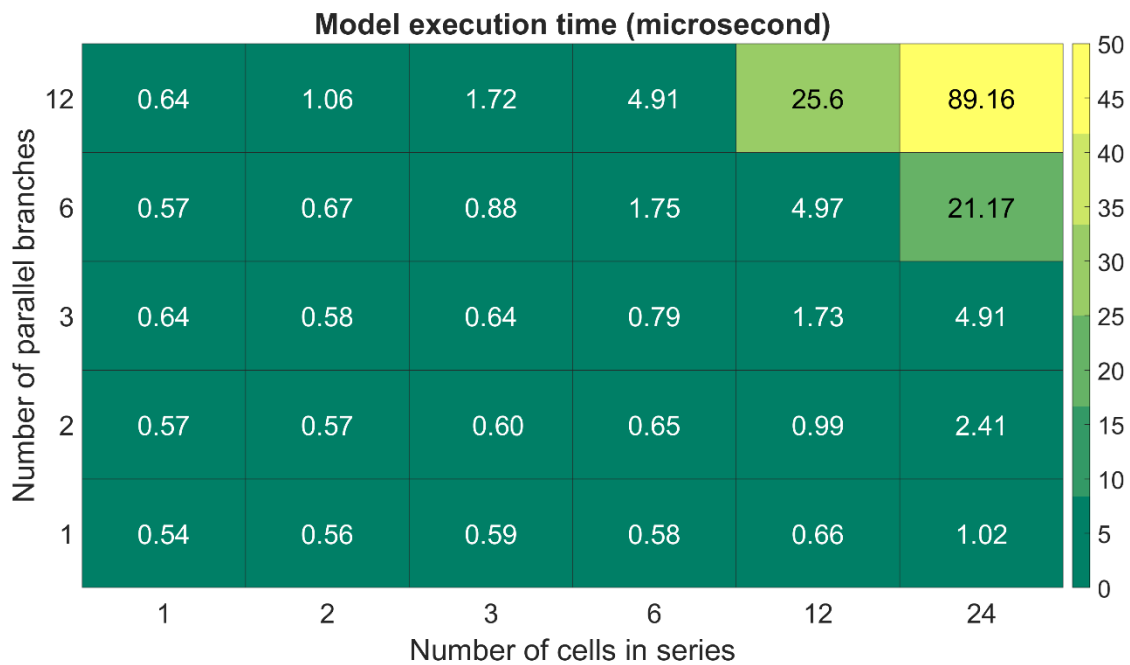
Figure 3.15 RC series model maximum execution times

From Figure 3.15 RC series model maximum execution times we can see that model execution times remains very low up to about 36 cells. and the values do not change significantly with the increasing number of cells, up to 36 cells. It is only the case of the 12x12 stack, the model requires a very much higher simulation step time. However, it must be remined that the RC series model has a very low model accuracy. The tables show three values for each test. 'm' represents the minimum execution time of the cycle, 'M' the maximum execution time of the cycle, and 'mean' the mean execution time.

Now let's move on to the analysis of the Two-Branch model.

	m M mean	m M mean	m M mean	m M mean	m M mean	m M mean
12	1.01 1.11 1.04	2.60 2.73 2.63	6.79 7.05 6.9	26.06 31.12 26.18	120.1 120.5 120.3	525.01 525.40 525.21
6	0.58 0.72 0.61	0.99 1.09 1.02	1.67 1.79 1.71	6.73 7.06 6.84	26.12 26.34 26.23	120.1 120.5 120.26
3	0.49 0.6 0.52	0.58 0.68 0.61	0.74 0.9 0.79	1.70 1.82 1.74	6.78 7.09 6.9	26.02 31.7 26.61
2	0.49 0.56 0.51	0.53 0.64 0.56	0.61 0.7 0.64	1.02 1.12 1.05	2.7 2.84 2.74	11.72 12.06 11.91
1	0.49 0.58 0.5	0.49 0.61 0.53	0.49 0.59 052	0.62 0.72 0.66	0.99 1.09 1.02	2.66 2.75 2.69
	1	2	3	6	12	24

Number of parallel branches (vertical axis label)

Number of cells in series

Table 3.3 The model execution times for supercapacitors stacks using the Two-Branch model.

■ 10e-5 stepTime ■ 50e-5 stepTime ■ 100e-5 stepTime ■ 300e-5 stepTime

■ 500e-5 stepTime □ 1000e-5 stepTime

Model execution time (microsecond)

Number of parallel branches \ Number of cells in series	1	2	3	6	12	24
12	1.10	2.73	7.05	31.12	120.50	525.40
6	0.72	1.09	1.70	7.06	26.24	120.50
3	0.60	0.68	0.90	1.82	7.09	31.7
2	0.56	0.64	0.70	1.12	2.84	12.06
1	0.58	0.61	0.59	0.72	1.09	2.75
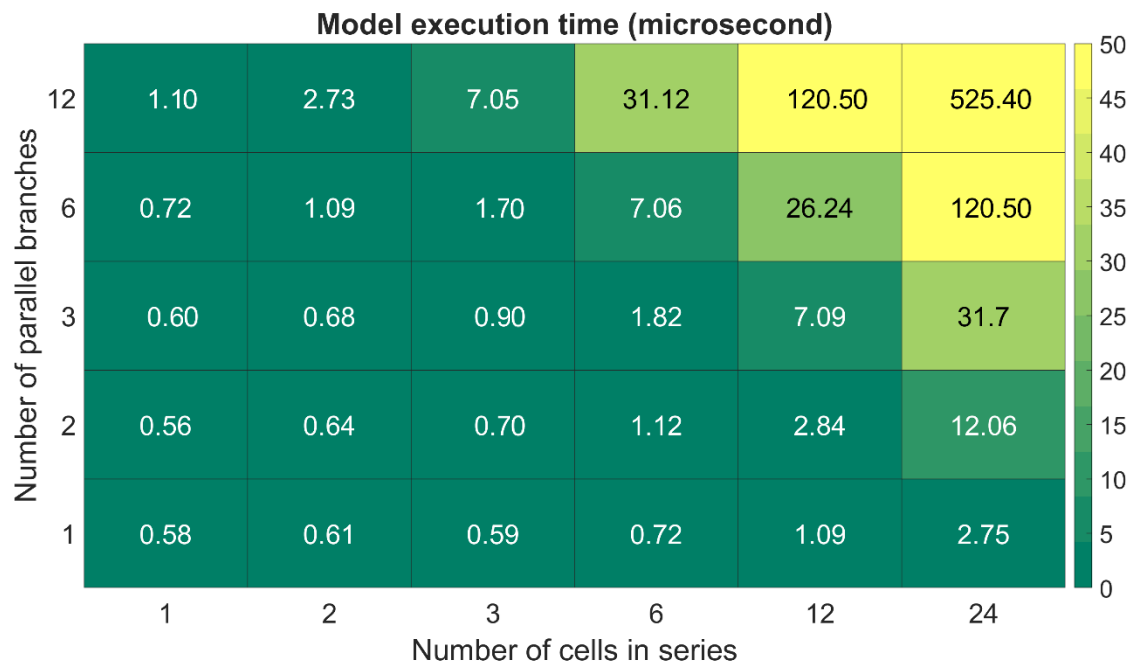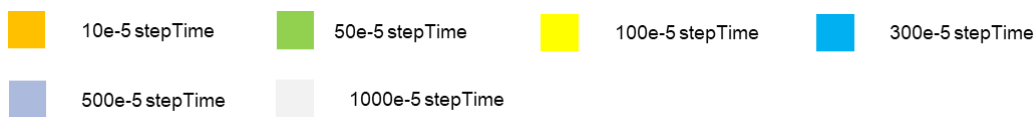
Figure 3.16 Two-Branch model maximum execution times

For the Two-Branch model the times are slightly higher than the RC model, as the model is more complex and contains parameters that vary with the voltage. Note that up to 6x12 cells, model execution time remains below the 50-microsecond threshold and is around 27μs. It is not possible to represent as many cells as with the RC model; however, the accuracy of this model is much better. Generally, in industrial applications 6x12 cells is sufficient so it can be said that the model is adequate for most applications. In this way, from Equation 1.3 and assuming 6 cells in series, 12 parallel branches, Vn=2.7V and C=3000F:

$$\Delta W = \frac{1}{2}CV_n{}^2 - \frac{1}{2}CV_{min}{}^2 \approx 590 \ kJ \qquad\qquad 3.1$$

The total power calculated assuming P≈300W for every cell is

$$P_{total} \approx 21.6 \ kW \qquad\qquad 3.2$$

Note that in Figure 3.16 the value grows beyond 500μs for a 24x12 stack, that is 10 times the threshold. The difference with the previous model is clear. It is possible to observe from Figure 3.16 that there is a sort of symmetry in the results. In fact, what affecting the response of the models is the number of cells. The structure of the stack is not affecting the results.

The Table 3.4 Zubieta model real-time simulation valuescontains the values of the Zubieta model. The two models are not very different so similar values are expected. As previously mentioned, the values of the times increase with increasing number of cells. In fact, it is possible to notice a sort of symmetry in the table: moving from the bottom left corner to the upper right corner the times always increase.

	m M mean	m M mean	m M mean	m M mean	m M mean	m M mean
12	1.53 1.65 1.57	5.43 5.61 5.51	13.65 13.77 13.69	56.51 56.71 56.59	254.51 255.12 254.85	>500 >500 >500
6	0.73 0.83 0.78	1.48 1.61 1.52	2.98 3.11 3.02	13.62 17.62 13.71	56.46 60.62 56.70	254.51 255.08 254.78
3	0.54 0.66 0.6	0.72 0.83 0.75	1.12 1.25 1.16	2.96 3.22 3.01	13.66 18.65 13.71	56.5 60.54 56.7
2	0.57 0.69 0.61	0.59 0.69 0.62	0.74 0.88 0.78	1.50 1.64 1.55	5.53 5.54 5.52	24.03 28.16 24.14
1	0.48 0.65 0.52	0.56 0.65 0.59	0.57 0.70 0.60	0.73 0.82 0.75	1.49 1.60 1.53	5.49 5.64 5.54
	1	**2**	**3**	**6**	**12**	**24**

Number of parallel branches (row axis) — Number of cells in series (column axis)

Table 3.4 Zubieta model real-time simulation values

Legend: 10e-5 stepTime | 50e-5 stepTime | 100e-5 stepTime | 300e-5 stepTime | 500e-5 stepTime | 1000e-5 stepTime

It can be seen at a glance that the difference between the two models are not significant. The representation possible with the Zubieta model is possible up to a lower number of cells. In fact, at 36 cells, the execution time begins to exceed ten microseconds, and at 6x12 cells it exceeds (even if
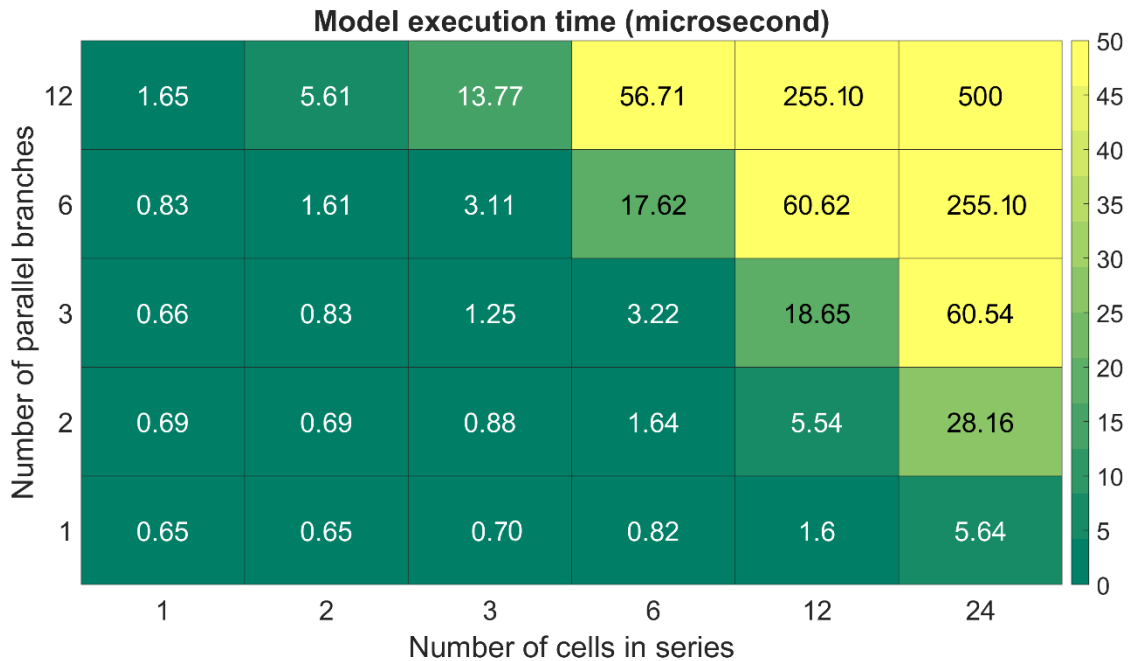

Model execution time (microsecond)

Figure 3.17 Zubieta model maximum execution times

only slightly) the threshold of 50µs. The value then rises to around 250µs with 144 cells. However,

one must keep in mind that our analysis showed that the Zubieta model does not necessarily increase

the model accuracy, when compared to the Two-Branch model.

Table 3.5 shows results for the Series model.

	m M mean	m M mean	m M mean	m M mean	m M mean	m M mean
12	202.48 203.88 203.15	444.58 458.85 450.33	720.55 739.5 728.23	1501.14 1542.01 1518.91	3220.52 3347.98 3274.27	> 8000 > 8000 > 8000
6	99.72 105.72 100.63	188.61 199.92 193.63	315.69 324.03 320.79	619.65 640.17 631.04	1704.41 1741.50 1724.61	3376.66 3728.8 3574.65
3	48.27 53.46 48.82	93.82 95.60 94.64	146.56 158.45 151.87	302.29 315.29 310.22	770.23 809.46 793.29	1885.18 1992.18 1941.10
2	34.44 35.03 34.66	61.93 63.10 62.5	93.15 95.22 94.08	186.82 194.3 191.47	469.46 483.83 476.09	1896.05 2025.73 1960.5
1	18.06 19.06 18.26	26.22 35.23 29.85	43.42 49.27 41.55	82.88 84.09 83.45	180.94 182.64 181.64	452.16 458.45 455.17
	1	2	3	6	12	24

Number of parallel branches (left axis label)

Number of cells in series

Table 3.5 The Series model execution times for supercapacitors stacks using the series model

- 🟧 10e-5 stepTime
- 🟩 50e-5 stepTime
- 🟨 100e-5 stepTime
- 🟦 300e-5 stepTime
- ⬜ 500e-5 stepTime
- ⬜ 1000e-5 stepTime

Model execution time (microsecond)

Number of parallel branches	1	2	3	6	12	24
12	203.90	458.90	739.50	1542	3348	8000
6	105.70	199.90	324	640.20	1742	3729
3	53.46	95.60	158.40	315.30	809.50	1992
2	35.03	63.10	95.20	194.30	483.80	2026
1	19.06	35.23	49.27	84.09	182.60	458.40

Number of cells in series
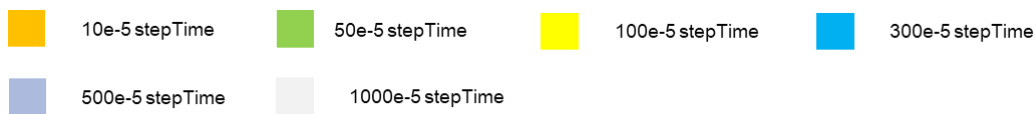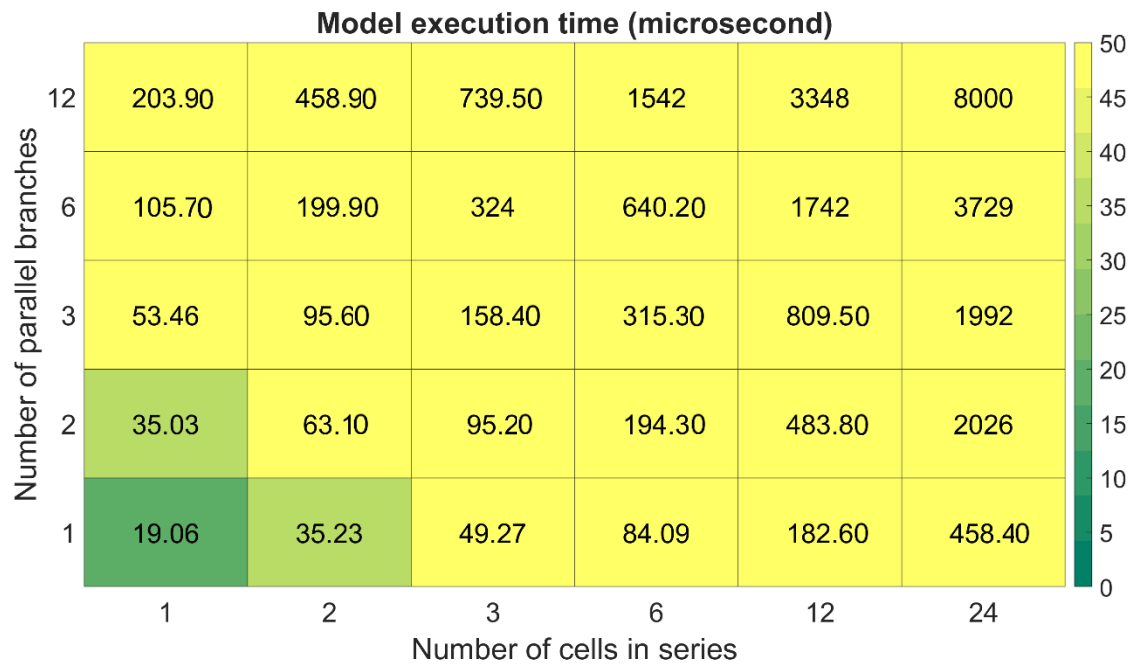
Figure 3.18 Series model maximum execution times

Here it is obvious that the model execution time is higher than 50 microseconds from 4 cells onwards. Clearly, this model is too heavy for a real-time simulation of a supercapacitor stacks. The step-times of the models have been adapted, as simulations were performed as time grew and values created. For the latest simulations of this model the value was in the order of milliseconds which is an unacceptable value, in terms of model accuracy.

4 Chapter 4: Summary and Conclusions

In this thesis, various supercapacitor models have been compared according to their accuracy and their required execution time for real-time simulations. It has been shown the the behavior of the supercapacitor can be represented accurately by some specific models, but not all models are suitable for real-time simulations.

The RC model proved itself to be extremely light for real-time simulations, but also extremely inaccurate with increasing error in time. In fact, after each cycle the error between the simulation model and the actual supercapacitor response increases drastically, leading to a very inaccurate result. The simplicity of the model allows for real-time representation of a very large number of cells, but its inaccuracy makes it unusable.

The Two-Branch model has been shown to be have highest accuracy together with an acceptable execution time for real-time simulations. There are other models that can represent the supercapacitor in more detail but, as far as the real-time representation of the component is concerned, it is the most performing one. In fact, the model has several advantages such as high accuracy, good response times and relatively simple implementation. The model therefore proves to be optimal in both terms of accuracy and execution time. In terms of accuracy, if subject to charge / discharge cycles in the order of tens of seconds, the model can accurately replicate the real behavior of a supercapacitor.

The model is not the only one to have correctly represented the voltage across the component therefore it must be said that different configurations can also be used as long as all the characteristics are taken on.

Among the analyzed models the series model has been proved to be the most accurate one, but also the most complex from the point of view of implementation as well as required execution time during real time simulations. Therefore, despite the fact that model can represent the fast dynamics of the circuit, remains extremely complex and therefore not suitable for real-time simulations.

The Zubieta model, which is just a variation of the Two-ranch model, has greater complexity and does not bring particular benefits from the point of view of accuracy. Although this model can also represent the supercapacitor response, it is slightly heavier than the Two-Branch model for real-time simulations, which increases in execution times.

In conclusion, the two-branch model is the best model for real-time simulation of large number of supercapacitor cells and it can represent such systems with a high accuracy and acceptable execution time.

Bibliography

[1]   A. Berrueta, A. Ursua, I. S. Martin, A. Eftekhari, and P. Sanchis, "Supercapacitors: Electrical Characteristics, Modeling, Applications, and Future Trends," *IEEE Access*, vol. 7, pp. 50869–50896, 2019, doi: 10.1109/ACCESS.2019.2908558.

[2]   S. R. Vosen and J. O. Keller, "Hybrid energy storage systems for stand-alone electric power systems: Optimization of system performance and cost through control strategies," *Int. J. Hydrogen Energy*, vol. 24, no. 12, pp. 1139–1156, 1999, doi: 10.1016/S0360-3199(98)00175-X.

[3]   S. Pay and Y. Baghzouz, "Effectiveness of battery-supercapacitor combination in electric vehicles," *2003 IEEE Bol. PowerTech - Conf. Proc.*, vol. 3, pp. 728–733, 2003, doi: 10.1109/PTC.2003.1304472.

[4]   P. J. Hall and E. J. Bain, "Energy-storage technologies and electricity generation," *Energy Policy*, vol. 36, no. 12, pp. 4352–4355, 2008, doi: 10.1016/j.enpol.2008.09.037.

[5]   A. Etxeberria, I. Vechiu, H. Camblong, and J. M. Vinassa, "Hybrid energy storage systems for renewable energy sources integration in microgrids: A review," *2010 9th Int. Power Energy Conf. IPEC 2010*, pp. 532–537, 2010, doi: 10.1109/IPECON.2010.5697053.

[6]   M. Conte, "Supercapacitors technical requirements fornew applications," *Fuel Cells*, vol. 10, no. 5, pp. 806–818, 2010, doi: 10.1002/fuce.201000087.

[7]   L. Shi and M. L. Crow, "Comparison of ultracapacitor electric circuit models," *IEEE Power Energy Soc. 2008 Gen. Meet. Convers. Deliv. Electr. Energy 21st Century, PES*, pp. 1–6, 2008, doi: 10.1109/PES.2008.4596576.

[8]   R. Faranda, "A new parameters identification procedure for simplified double layer capacitor two-branch model," *Electr. Power Syst. Res.*, vol. 80, no. 4, pp. 363–371, 2010, doi: 10.1016/j.epsr.2009.10.024.

[9]   L. Zubieta and R. Bonert, "Characterization of double-layer capacitors for power electronics applications," *IEEE Trans. Ind. Appl.*, vol. 36, no. 1, pp. 199–205, 2000, doi: 10.1109/28.821816.

[10]   V. Musolino, L. Piegari, and E. Tironi, "New full-frequency-range supercapacitor model with easy identification procedure," *IEEE Trans. Ind. Electron.*, vol. 60, no. 1, pp. 112–120, 2013, doi: 10.1109/TIE.2012.2187412.

[11]   M. D. Omar Faruque *et al.*, "Real-Time Simulation Technologies for Power Systems Design, Testing, and Analysis," *IEEE Power Energy Technol. Syst. J.*, vol. 2, no. 2, pp. 63–73, 2015, doi: 10.1109/jpets.2015.2427370.

[12]   F. Adler, A. Benigni, H. Stagge, A. Monti, and R. W. De Doncker, "A new versatile hardware platform for digital real-time simulation: Verification and evaluation," *2012 IEEE 13th Work. Control Model. Power Electron. COMPEL 2012*, pp. 1–8, 2012, doi: 10.1109/COMPEL.2012.6251742.

Notes of Thanks

I would like to dedicate a few lines to the people who have supported me on this path. In particular I would like to thank my family, who have always been close to me. I thank my brothers who have given me great support, each in their own way. I thank my girlfriend and friends who have always been close to me.

A special thanks goes to Bea, who has always supported, forgiven and given me all her affection, showing me every moment that she was there beside me.